

New Results on RF and DC Field Emission

H. Padamsee, J. Kirchgessner, D. Moffat, R. Noer,
D. Rubin, J. Sears and Q. S. Shu

Laboratory of Nuclear Studies, Cornell University, Ithaca, NY 14853

1.0 Introduction

This paper will review progress in RF and DC field emission since the last workshop held 2 years ago at Argonne National Laboratory[1]. Through better characterization, progress has been made towards improved understanding of FE in cavities. Through development of new cures, gains have made towards higher fields. Through better rinsing procedures low-frequency (500 and 350 MHz) cavities regularly reach surface electric fields of 20 MV/m. Processing times are substantially reduced. Through heat treatment at 1350°C high frequency (1500 MHz) cavities have reached 53 MV/m and 3000 MHz cavities have reached 70 MV/m.

2.0 State of the Art in E_{pk}

Surface electric fields achieved in the last few years by various laboratories [2-8] with accelerating structures and single cell cavities designed for electron acceleration are shown in Figure 1. We view performance in terms of the cavity surface area, as past experience has

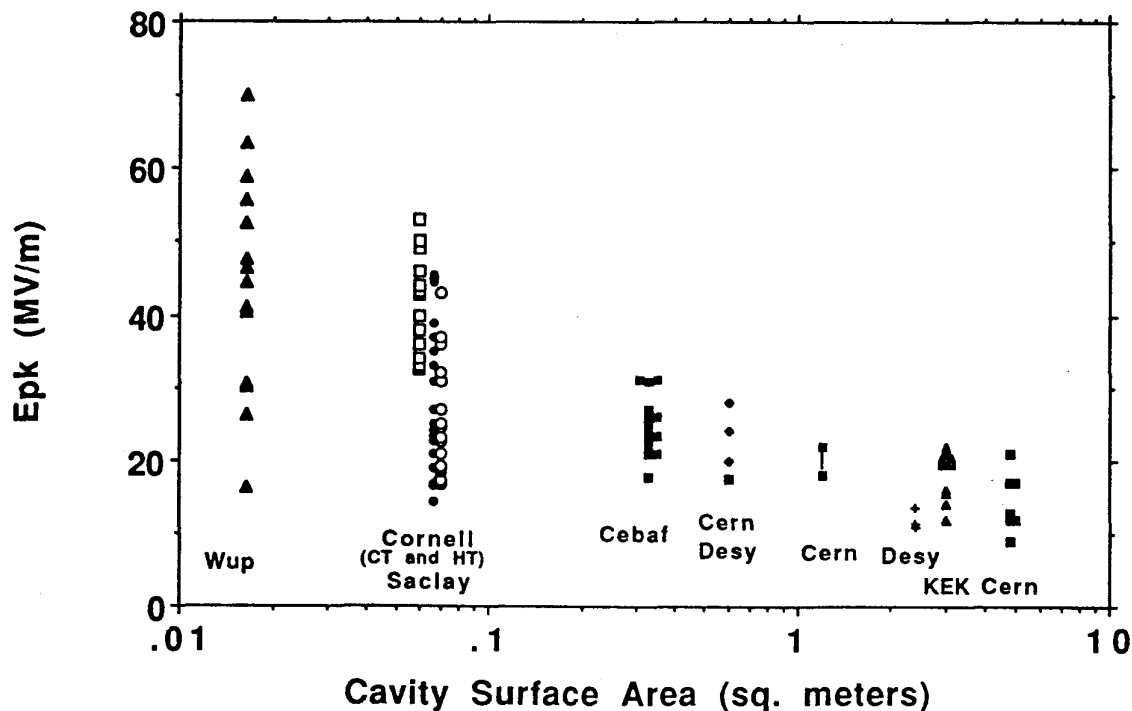


Fig. 1 Survey of recent achievements in 1-cell cavities and accelerator structures by various laboratories involved in the development of Nb cavities for electron accelerators.

shown that the number of emitters (and defects) increases with area. In-beam tests are excluded from this comparison for two main reasons: not all organizations have evaluated in-beam operation; secondly, assembly for in-beam operation will likely introduce further contaminants (emitters) until experience improves. We expect that eventually in-beam tests will approach the laboratory test levels as experience in large-scale installations continues. The Nb for all the cavities reported here had $RRR > 120$ (see Table 1). The majority of cavities were prepared with chemical treatment based on a buffered acid dip. Only KEK uses a different chemistry, based on electropolishing. Cavities heat treated above 1100°C are also shown here, and will be discussed in more detail in another section. In most cases the field limits are from field emission, although the few reported quench cases are also included.

These results show substantial progress over the state of the art as first summarized (Fig. 2 (a)) in a similar fashion at the first SRF workshop held in 1980[9]. Maximum field levels of 1980 are superposed as a dashed line with the present state of the art in Fig. 2 (b). Around and below 1500 MHz, a factor of 3 improvement has been realized in this decade. It is encouraging that surface electric fields near 20 MV/m are regularly achieved today in cavities with more than 1 m^2 surface area. Remarkably,

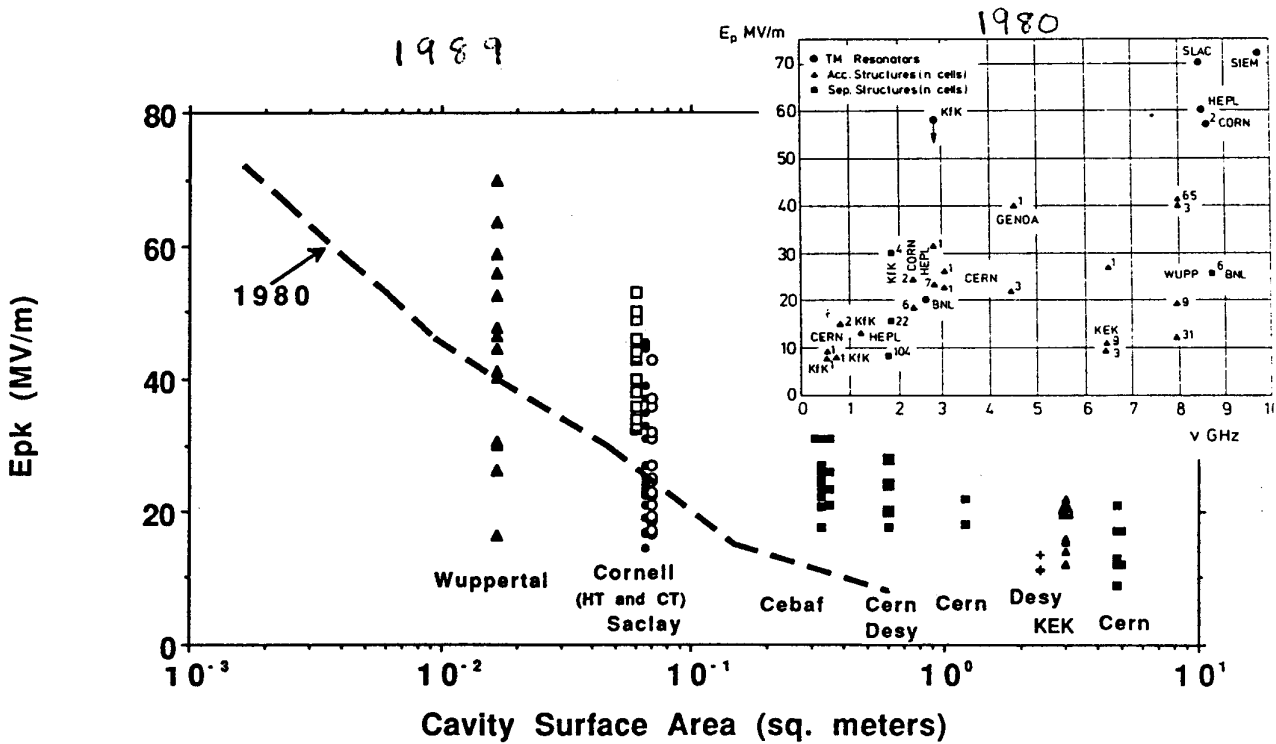


Fig. 2 A comparison of the state of the art 1989 to 1980 (inset). The dashed line in the 1989 portion represents the best 1-cell performance of 1980 after conversion of 1980 frequency axis to surface area.

performance drop appears to level off above 1 m^2 . Improved rinsing after chemical treatment is believed largely responsible for the high fields reached in large-area structures. At 3 GHz there is a 75% improvement (we discount the one point that is reported to be transitory, as indicated by the downward arrow). Electric field values $>60 \text{ MV/m}$ that in the past were only achievable in 8-10 GHz cavities are today exceeded at 3 GHz and approached at 1.5 GHz. Whereas surface magnetic fields $>1000 \text{ Oe}$ were considered landmarks achieved occasionally in X-band resonators, today they are routinely exceeded in 1.5-GHz and 3-GHz single cells.

Among the most basic questions pertaining to the high-field capability of Nb cavities is whether a Nb surface under any condition will tolerate surface RF electric fields above the record 70 MV/m of Fig. 2. A Nb accelerator cavity operating near the theoretical limit set by critical magnetic field (2000 Oe) needs to support a surface electric field of $\sim 100 \text{ MV/m}$. DC electric fields as high as 200 MV/m have been achieved over cm^2 Nb surfaces. Accelerator cavities have large areas simultaneously exposed to high electric fields, so that emission from a few spots limits application of higher fields elsewhere, even though other areas may have the higher intrinsic capability.

To determine the intrinsic capability of Nb surfaces with regard to high RF electric fields, a new "mushroom" cavity has been designed and tested at Cornell (see Fig. 3). A complete discussion of the development and experiments with this cavity is given in another paper at this workshop[10]. Here we summarize the salient result.

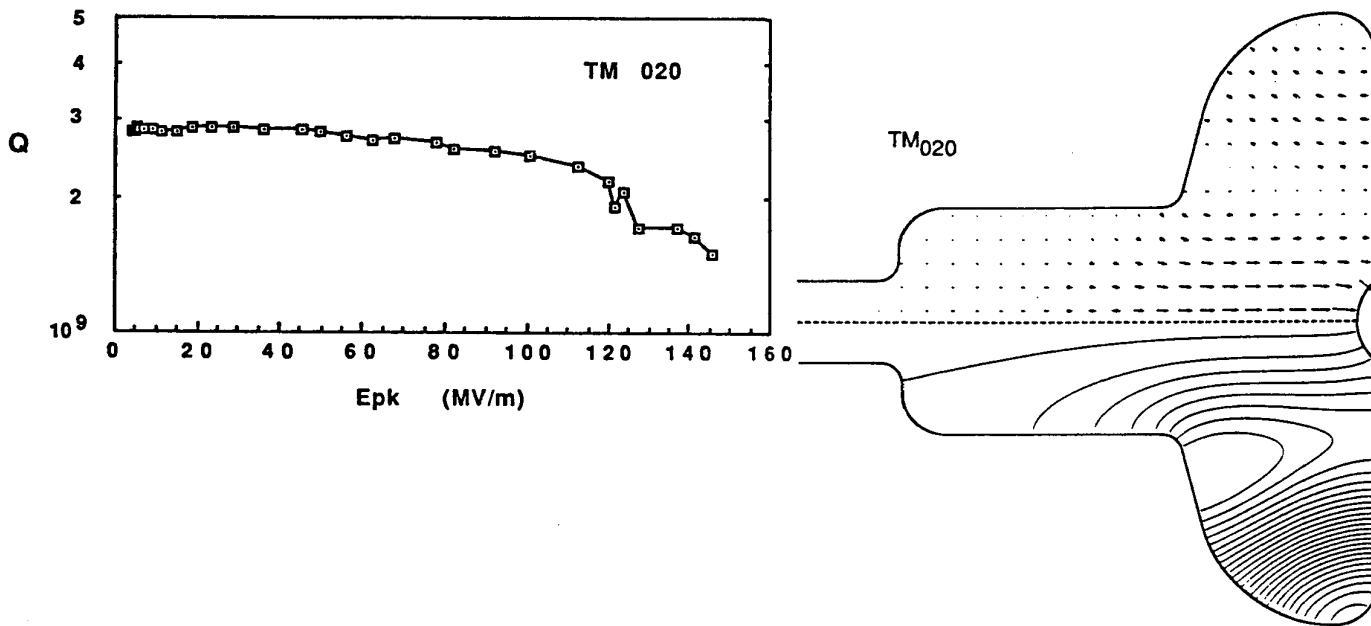


Fig. 3 (a) Electric field representations from URMEL for the "mushroom" cavity. The upper half shows equipotential lines in $rH\phi$ and the lower half shows the electric field.
 (b) Best performance of the mushroom cavity.

A standard S-band accelerator cavity half cell is closed off at the equator with a Nb plate. In a non-accelerating higher mode, the center of the plate has a very small area exposed to electric fields. A small dimple is placed at this high-field location to further enhance the electric field. Typically the field falls to 80% of the maximum value within 10 mm² of the dimple center. The maximum electric field is 5 times higher than anywhere else on the cavity surface outside the dimple. The cavity also has very favorable ratio of peak surface electric to peak surface magnetic field. For 100 MV/m at the center of the dimple, the highest surface magnetic field is 930 Oe, well below the theoretical limit of 2000 Oe.

After overcoming initial difficulties, we succeeded in reaching a Q value of 3×10^9 at low fields, and a maximum field of 145 MV/m with a Q value above 10^9 . We did observe emission but we suspect that it originated from a lower field region around 30 MV/m, where the area and probability of encountering emitters is significantly greater. We have thus established that there are no fundamental limits to reaching the desired RF electric fields of 100 MV/m on Nb surfaces. The high-field area in the mushroom cavity is equivalent to that of a TM010-mode accelerator 1-cell cavity at 35 GHz.

A similar cavity at 3.5 GHz is under development by the Wuppertal/Saclay collaboration[11].

3.0 Benefits of High Temperature Treatment

Motivated by the success at the U. of Geneva in reducing DC field emission by heat treatment of Nb surfaces[12], exploration of the influence of high temperature annealing[4] in the final stages of rf cavity surface preparation has continued.

At the time of the last SRF workshop we reported on results from two heat treatments of 1.5-GHz single cells and compared these with results from chemical treatment. We showed that at 20-24 MV/m, heat treatment of 1100-1200°C resulted in almost no emitters on the RF surface in the virgin condition, i.e., without any processing. In comparison, chemically treated surfaces which reached this field level after He processing showed many strong emission sites. By now we have carried out 15 separate heat treatments on 7 different cavities (1.5-GHz, 1-cell). As a control, as well as to gain more data on emitter statistics and properties, we conducted additional tests with chemical treatment over the same time period as the heat treated cavities. As discussed below, we find that higher temperatures and longer times are more effective in reducing FE. We have also found that during removal of the cavity from the furnace, additional dust contamination is inevitable. To overcome this problem we rinse cavities with clean methanol just before attachment to the RF test station. Accordingly we present the heat treated cavity results in three categories:

- (A) Highest temperature heat treatment & rinsed
- (B) Medium temperature treatments & rinsed and
- (C) Medium temperature treatments & not rinsed.

The results of the most recent chemical treatments are presented in comparison with the heat treatments of category (A).

During the RF tests we utilized a high speed/superfluid-He temperature mapping system to locate and analyze the FE sources from the power deposited on the cavity surface by emitters in an RF field. In this system 684 carbon thermometers are affixed to the cavity so that each resistor is in thermal contact with the outer wall of the cavity. The large number of fixed thermometers ($1/\text{cm}^2$) allows us to scan the entire surface of the cavity in 15 seconds as opposed to the older technique of mechanically moving a smaller array over the cavity surface which takes 30 minutes. The high speed makes it possible to study local heating as a function of field level or of time. The high heat-transfer coefficient of superfluid He as well as the absence of BCS losses at 1.5 K increases the temperature stability of the RF surface at high RF fields. As an added benefit, the spatial resolution of the superfluid thermometry is increased by a factor of 2.5 over 1st generation subcooled He thermometry, helping to better pinpoint the location and number of emitters. However, the sensitivity is reduced from near 100% of the wall temperature rise to about 30%. The system was described in detail in [13] and at the last workshop[14].

A movable superfluid He temperature mapping system has been developed by the Wuppertal/Saclay collaboration and used to locate dominant emitters in their cavities[7]. The sensitivity (1-2 % of the wall temperature) is less than that of the fixed system due to the absence of grease that promotes thermal contact between the sensor and the cavity wall. The thermometer response is found to be non-linear with power so that more elaborate calibrations are necessary. This system also includes a movable X-ray detector array placed adjacent to the cavity. Correlated signals from temperature and X-ray mapping systems show the consistency of locating emitters by thermometry techniques.

3.1(A) Highest Temperature (1300-1350°C) Treatment/

Comparison with Chemical Treatment.

Four heat treatments were carried out at 1300-1350°C, for periods between 4-8 hours. Five RF tests were conducted on these cavities. We estimate the RRR of the cavity wall to be ~ 400 from monitor samples placed in the Ti box in such a way that only one side was coated with Ti.

Figure 4 compares the Q vs E_{pk} behavior from tests after the highest temperature treatments with that of the more recent chemical treatment tests carried out as control experiments. In all cases shown, results are

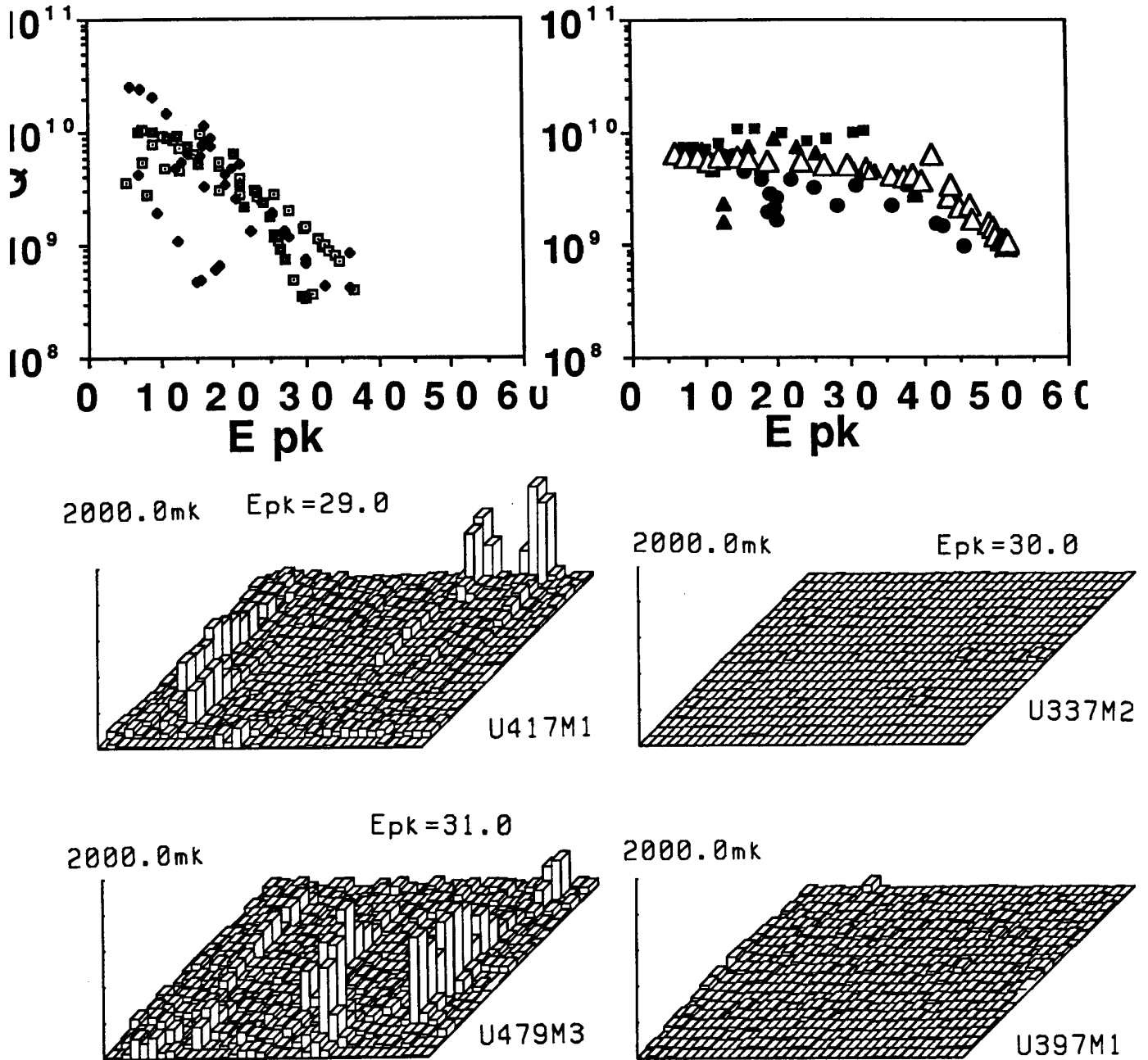


Fig. 4 Reduction of FE with heat treatment at 1350 C (right half) as compared to standard chemical surface treatment (left half). Q vs E curves in the uppermost figures are for 3 separate chemical treatments (left half) and for 4 separate heat treatments and 5 tests (right half). Temperature map comparisons at $E_{pk} = 30$ MV/m for separate tests of each type of treatment show the substantial reduction in emitter density. Results in all cases are for the "virgin" surface, ie no RF or He processing was attempted.

for the virgin RF surface--i.e., on first raising the RF power. Such a comparison is a more demanding evaluation of the benefits of a new procedure. On the left side of Fig. 4, results from chemically treated cavities are shown, in contrast with those of the heat treated cavities on the right side. In several cases a few emitters which appeared below 30 MV/m processed away rapidly with increases in RF power. Emission properties of a few of these rapidly processed sites were successfully analyzed and will be discussed later. Representative temperature maps taken near 30 MV/m are shown in the lower part of the figure. Many strong emitters are present in each of the chemically treated cases, whereas the heat treated surfaces are virtually free of emitters at 30 MV/m. In one of the HT cases the temperature rise due to a defect has been artificially suppressed in the figure, after positive identification from the typical linear increase in temperature rise with E^2 .

An important difficulty that arose during high-temperature treatment of cavities was that the RRR of Nb normally drops substantially (to < 100) due to absorption of oxygen into the bulk from the residual gases in the furnace. To overcome this problem we devised the special procedure sketched in Figure 5[4].

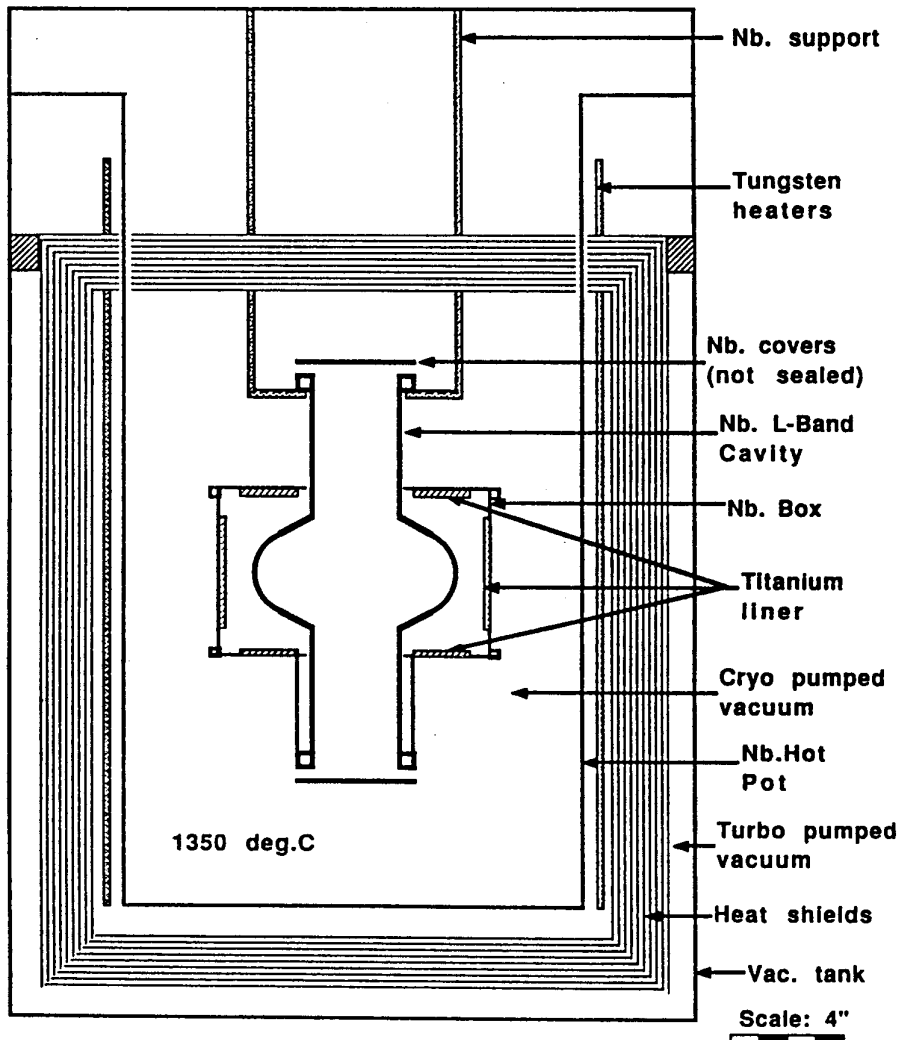


Fig. 5 Protection with Ti against RRR drop during heat treatment above 1300 C.

Ti sheets surround the outside of the cavity. Evaporated Ti forms a protective film against gases which strike the outer cavity wall. Gases striking the inside (RF) surface diffuse rapidly to the outer wall and are removed from the Nb by the solid state gettering process at the Nb-Ti interface. To prevent Ti vapors from reaching the interior of the cavity, the Ti sheets are surrounded by an outer can of Nb, and the beam tube openings are baffled by Nb covers.

For 3 of the 5 HT tests, the Ti-rich layer on the outside was chemically removed while the cavity was filled with class-100 air and sealed so that the RF surface was not exposed to acids. (After chemistry, the RF surface was rinsed with methanol in ultrasound for 1/2 hour.) This additional step of outside chemistry is necessary to overcome a negative side effect from the presence of the ~25 μ m-thick Ti layer deposited on the outer wall of the cavity. Our temperature diagnostic system showed that this layer impedes heat flow to the He bath. If the Ti layer is left on, the temperature signals are enhanced by one order of magnitude and the power tolerable during subsequent processing to reach the highest field is restricted. In the RF tests following the outside chemistry, we found the cooling impedance to be eliminated as shown by the reduced temperature signals as well as by an increase in power tolerable during processing of FE.

Another negative side effect of Ti protection is that the Q of the cavity at low fields is somewhat lower than usual (5 - 7 $\times 10^9$ instead of our 1 - 2 $\times 10^{10}$) presumably due to some Ti deposition on the RF surface. The level of Ti is too small to definitively pick up on the SEM, but enough to be visible as equator heating in the temperature maps.

Emitter Properties

Temperature maps can be used to analyze Fowler-Nordheim (FN) properties of emitters. We begin by assuming that the current I (in A) emitted by a particular FE source is given by the modified FN relation:

$$I = [AS\beta E^2/\phi]\exp[-B\phi^{1.5}/\beta E).$$

Here the applied field E is in V/cm, $\phi = 4$ eV for Nb, $A = 1.54 \times 10^{-6}$ and $B = 6.83 \times 10^7$ are constants, S is the emissive area (cm²) and β is the famous FN field enhancement factor. By now it is well established that β and S are only parameters to express the emitted current; their physical significance is not yet understood. They are traditionally used to characterize emitter properties.

An electron emitted at a particular instant of the RF cycle from an assumed source at a particular location on the cavity wall will impact the wall at the same longitude as the source.

The point and energy of impact can be calculated from the electron dynamics in the known cavity fields. The deposited power density distribution arising from a time-varying current of these electrons, emitted according to the FN equation (assuming a particular β and S) can then be calculated. By smearing the power deposited on the inner wall (RF surface) to simulate heat flow through the Nb wall, one can also calculate the expected temperature map for the emitter. The thermometer response is calibrated in a separate apparatus against a known deposited power and is found to be linear with power over a wide range (50 μ K to 1K). The measured thermometer efficiency [13] is incorporated in the calculated temperature maps. Within reasonable limits, a good match can always be found between a measured temperature map and one of the calculated maps. From the position of the assumed emitter for this calculated map, we obtain the position of the real emitter. (In 1.5-GHz cavities, the calculated peak heating normally takes place near the emitter. Thus the approximate emitter location is obvious from the map.) From several ΔT maps calculated for a given hypothetical emitter over a range of E field values, we find that ΔT_{pk} (the peak ΔT at the longitude of the emitter) also follows a FN behavior--i.e., $\ln(\Delta T_{pk}/E^2)$ is linear in $1/E$, with a slope approximately equal to β . A corresponding series of experimental maps can therefore be used evaluate β . The β value is independent of thermometer calibration. The equivalent emissive area can be determined from the intercept of this line. Using emissive areas of 10^{-6} to 10^{-16} cm² we obtain intercept values for the ΔT -based FN plots from -10 to -33, which serves as a rough conversion for intercept to emissive area.

Figure 6 shows temperature maps for a cavity (CSI/F3) which was heat treated at 1350°C for 4 hours. Results reported are without He processing to show the behavior of the virgin surface. Two emitters processed rapidly

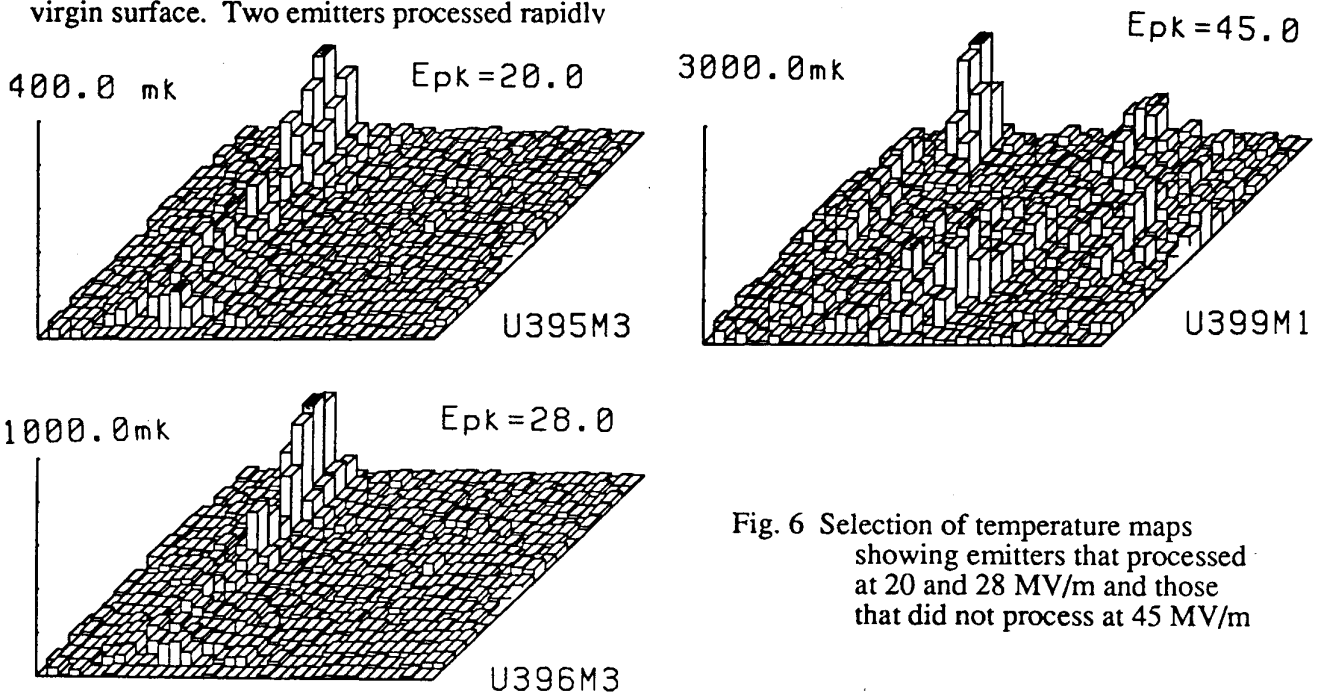


Fig. 6 Selection of temperature maps showing emitters that processed at 20 and 28 MV/m and those that did not process at 45 MV/m

at 20 MV/m and 28 MV/m, but several maps including maps (a) and (b) of Fig. 6 were nevertheless successfully captured while emission was in progress so that emitter properties could be analyzed. This is one of the important advantages of the rapid temperature mapping system. At 45 MV/m four long lasting emitters are clearly visible in map (c) of Fig. 6. Hot spots near the equator are defects, possibly from the slight Ti contamination of the RF surface. Other small hot spots which showed linear behavior in ΔT vs. E^2 have been ignored.

After this test, the cavity outside surface was chemically treated to remove the Ti layer as discussed above. The inside of the cavity was then rinsed once again with methanol and then the cavity was tested. No transient emitters were encountered and $E_{pk} = 51$ MV/m could be reached, at which stage the map in Fig. 7 was taken showing 5 strong emitters.

Analyzed properties of these and other emitters for similarly treated cavities were compiled. The β -intercept distribution is displayed in Figure 8(a). The envelope has the characteristic shape first reported in [15]. Absence of emitters below the envelope is expected as the emission current is too low to permit detection. However absence of emitters above the envelope needs explanation. We note that the two emitters which processed rapidly lie clearly outside the envelope described by the long-lasting emitters. Therefore it is reasonable to suppose that in general emitters lying above the envelope (ie in the direction of stronger emission) will process away more rapidly and thereby also escape detection.

High field maps for our control chemical treatment tests are shown in Figs. 4(a) and (b). These cavities showed two and three rapidly processed emitters before reaching 29 and 31 MV/m, respectively. The detailed properties of the emitters visible on the maps were analyzed. Corresponding β -intercept distribution is given in Figure 8(b). Once again we note that the rapidly processed emitters lie outside the envelope described by long-lasting emitters.

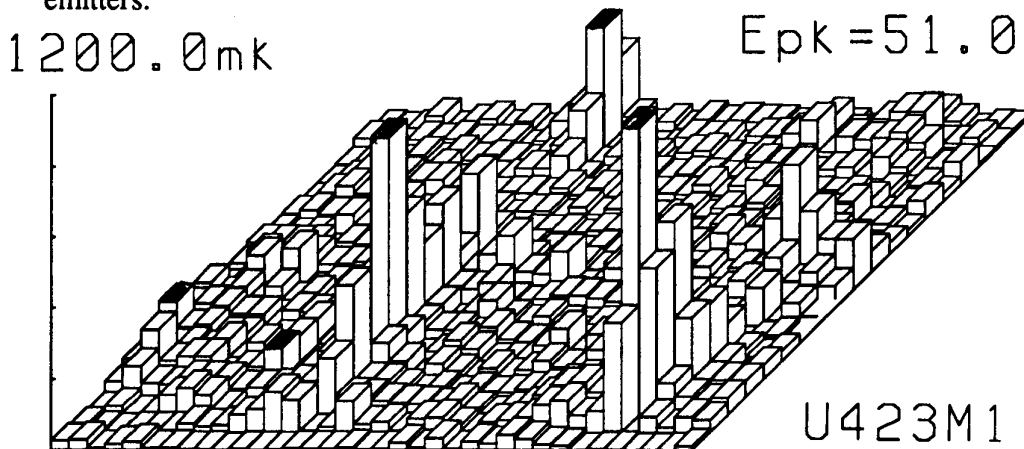


Fig. 7 Temperature map for a heat treated cavity at 51 MV/m showing three strong emitters and two weak ones.

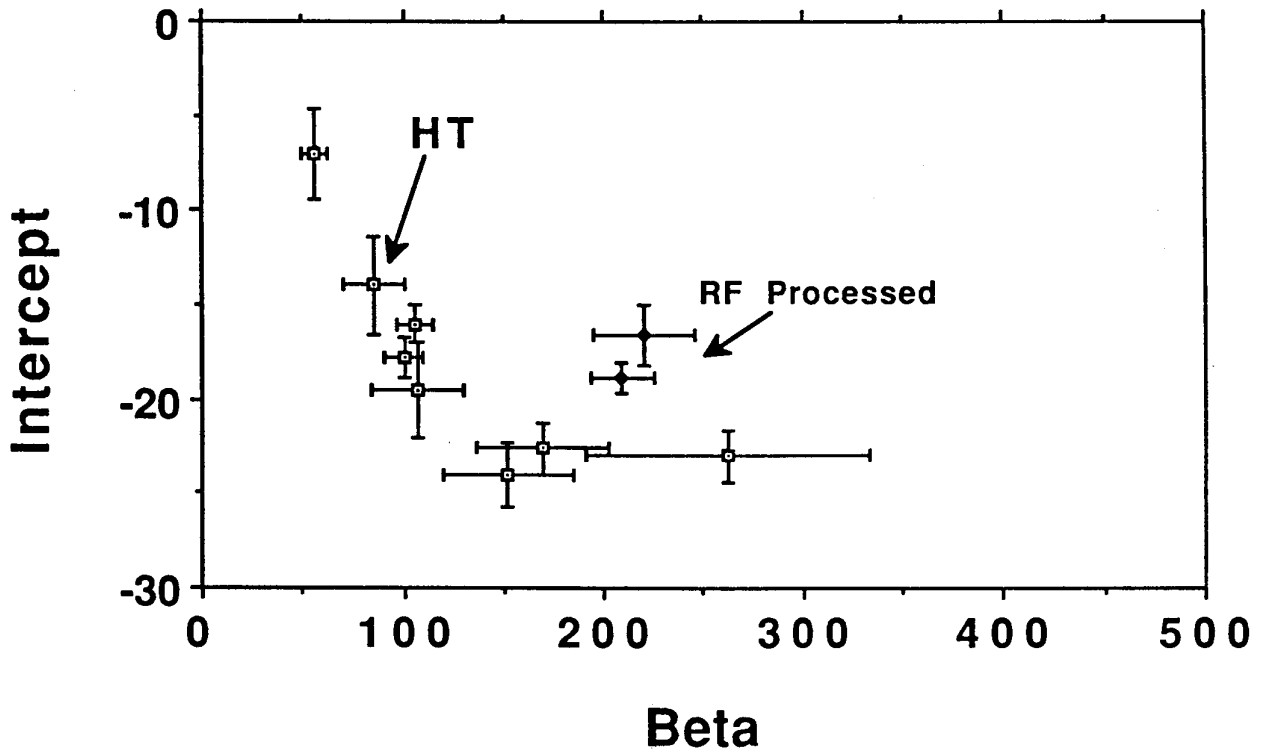
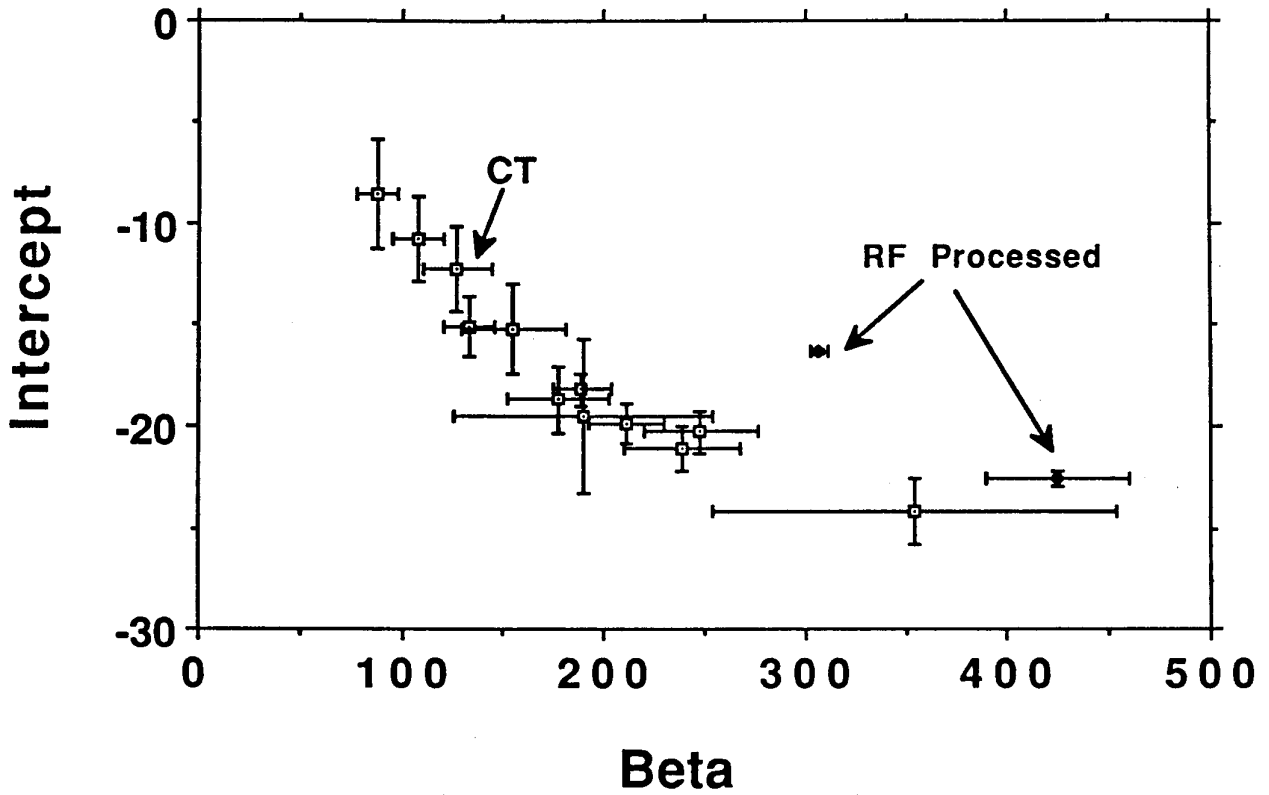


Fig. 8 Fowler Nordheim properties, β and $\log[\text{intercept}]$ for emitters on Nb surfaces prepared by (a) chemical treatment (CT) and (b) heat treatment (HT). The intercept values can be converted to emissive area using the relation $\log[\text{area}(\text{cm}^2)] = -1.65 + 0.44 \cdot \log[\text{Intercept}]$ derived from simulated temperature maps. Note that the two emitters that lie outside the envelope processed quickly.

A comparison of the β -area distributions for the heat treated and chemically treated surfaces given in Figure 8 shows clearly that the CT emitters are stronger. From the substantially different individual emissive properties, it is likely that the physical nature of sites characteristic of chemically prepared surfaces are different from those of sites typical of a heat treated surface.

Emitter Statistics

From temperature maps we can compile statistics on the numbers of emitters as a function of field. In the histograms to be presented below, we will associate an emitter with the highest field level at which it is apparent (this being either the maximum possible field for the surface condition under study or the highest field level at which the emitter was recorded before being processed away).

From the number of emitters that appear at given field levels, we constructed emitter frequency distributions for heat treated and chemically treated surfaces. 16 emitters were counted in the two CT tests (15 analyzed) and 14 emitters in four HT tests (10 analyzed). The results are plotted in Figure 9. Each distribution is consistent with an emitter density increasing exponentially with increasing field level. However there is a substantial reduction in the exponent for the heat treated surface. To convert emitter density/test to emitters/cm², we take as the effective cavity area that part of the surface on which the field maintains 80% of its peak value--53 cm² in a 1.5-GHz 1-cell cavity.

Recently CERN reported sighting 17 emitters at 12 MV/m (surface field) in a monocell 500 MHz cavity[16]. A test of the CERN cavity samples 9 times the surface area involved in our tests. Therefore the equivalent emitter density is 17/9 = 1.4 emitters/test, which is in agreement with our point of 1.5 emitters/test at 10-20 Mv/m for a chemically prepared surface.

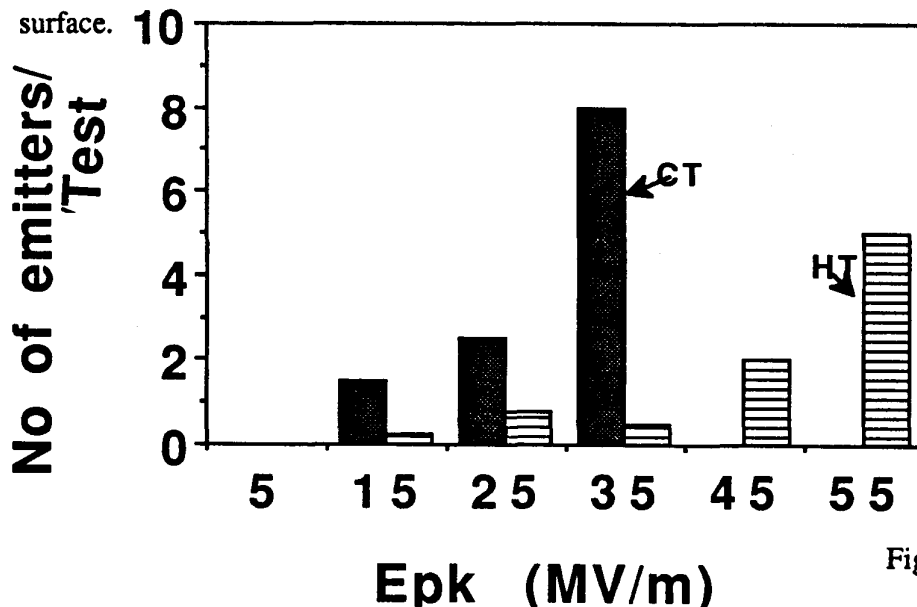


Fig. 9 Comparison of emitter density distributions for CT and HT surfaces.

Both β -intercept comparisons (Fig. 8) as well as emitter density distribution comparisons show that HT (1300-1350 C, 4-8 hrs) not only reduces the strength of emission sites but also their number density. World statistics on RF and DC [12] emitter densities for chemically treated surfaces are shown in Fig. 10. There is reasonable agreement between DC and RF emitter density distributions both for CT surfaces as well as for HT (1350 C) surfaces. About one order of magnitude drop is realized with HT. As discussed in the next section lower temperatures were less effective. We anticipate that a further drop in emitter density will be necessary to reach even higher fields. Therefore higher temperatures should be tried. In this case it may be necessary to replace the Ti protection with Zr protection because the vapor pressure of Ti may get too high for the furnace.

The behavior of highest-temperature HT cavities after He processing will be discussed in the section on He processing.

3.2 Intermediate Heat Treatments

These tests were conducted before development of the Ti protection to preserve RRR. Therefore the temperature was kept low or the time at the highest temperature was kept short. Five tests were conducted after HT at temperatures 1200-1250°C for 2-5 hours and one at 1350°C for 15 minutes. All cavities were rinsed with methanol after HT. We estimate the bulk RRR for the cavity wall after treatment to be between 130 and 260. This was obtained from change in RRR of monitor samples placed in the furnace aside the cavity.

As before we evaluate the behavior of the cavities without any He processing to assess the quality of the virgin surface.

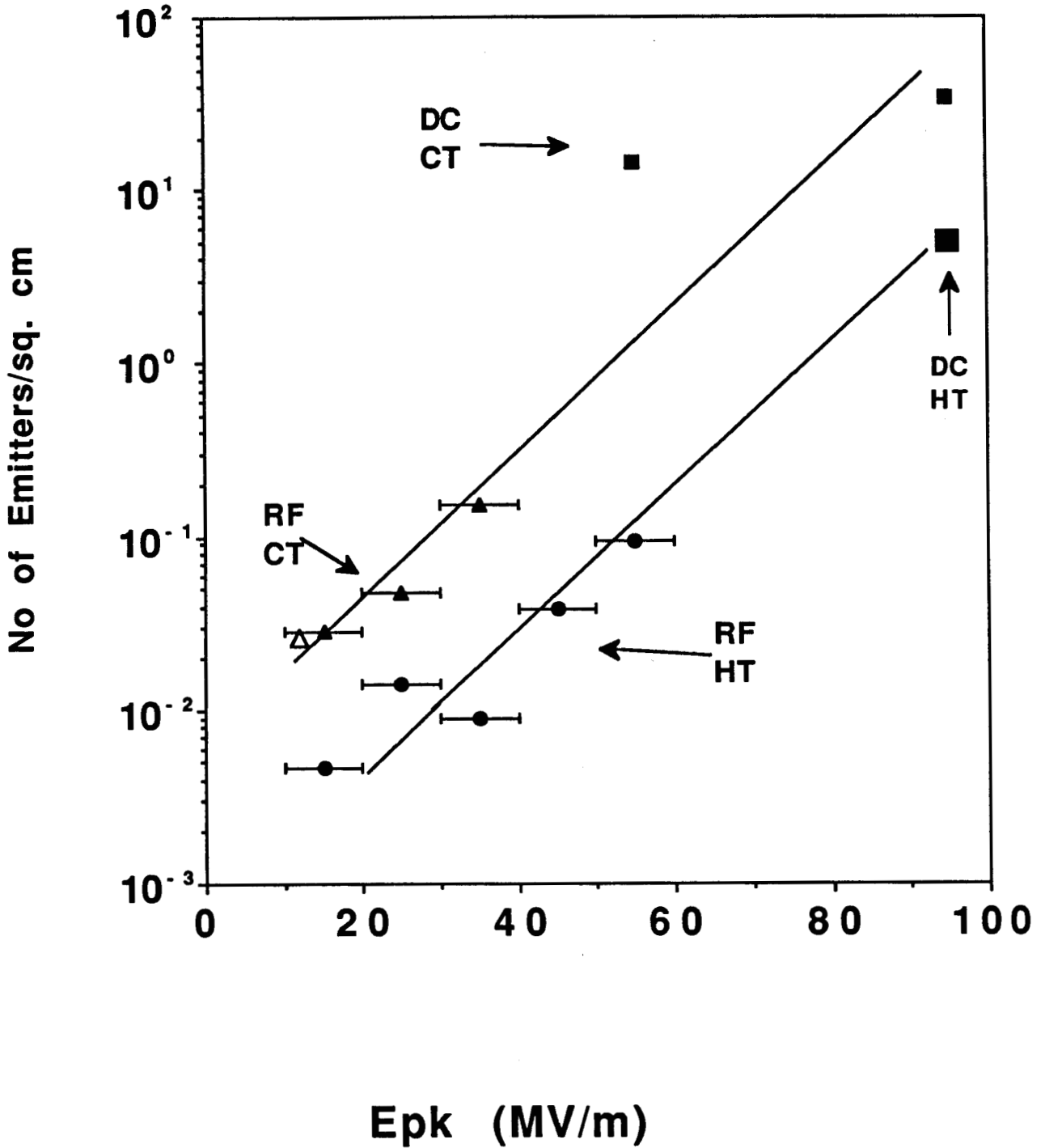


Fig. 10 Increase of RF and DC emitter densities with surface electric field for two different surface treatments, CT and HT ($T = 1350$ C). The open triangle is from CERN RF data[4]. The solid triangles are Cornell 1.5 GHz data and the solid squares are DC data[12], all for CT surfaces. The surface area for high E_{pk} for a 1.5 GHz cavity is 53 sq. cm and for the CERN cavity is 450 cm². The solid circles are for Cornell HT data and the large solid triangle is DC data at 90 MV/m [12]. Note the agreement between RF and DC densities.

Emitters that rapidly process with initial raising of RF power are also counted if they persist long enough to be captured with our fast temperature mapping system. Fig. 11(a) gives the Q vs E behavior of intermediate HT cavities. This can be compared with the most recent chemically prepared cavity tests as in Fig. 11(b). Thermal breakdown limited two tests due to the RRR drop during HT. Three tests showed strong emission. Fig. 12(a) shows the emitter distribution compared with that from the chemically treated cavity tests. Although there is an observable reduction in the emitter density, it is not as substantial as with the 1350°C HT for long times. Emitter properties are compared in Fig. 12(b) with emitters from CT tests and show no measurable difference. This is in strong contrast to emitter properties after 1350°C HT.

In summary intermediate heat treatments were not as effective in reducing FE as 1350 C for 4 hours or longer. Emitter densities were reduced from the chemically treated case and the emitters properties were favorably influenced by He processing.

3.3 Heat Treatments Without Final Methanol Rinsing.

Three cavities were heat treated at intermediate temperature and tested without rinsing with methanol. Q vs E curves are given in Fig. 13(a) and can be compared with CT cavities of Fig. 11(b). Emission is slightly stronger than for CT cavities. The emitter distribution density is shown in Fig. 14(a) and is found somewhat higher than with CT cavities. Emitters were analyzed and their properties are compared in Fig. 14(b) with emitters from CT cavities. Larger β values are systematically present. All results suggest that the contamination introduced during the introduction and removal of the cavity from the furnace was serious. Fortunately dust-free methanol does not increase emission, as discussed later and presented in more detail in another paper at this workshop. Therefore rinsing after firing is recommended, unless improved handling procedures can be developed in the future. The latter may become necessary if higher temperature treatment gives even better surfaces.

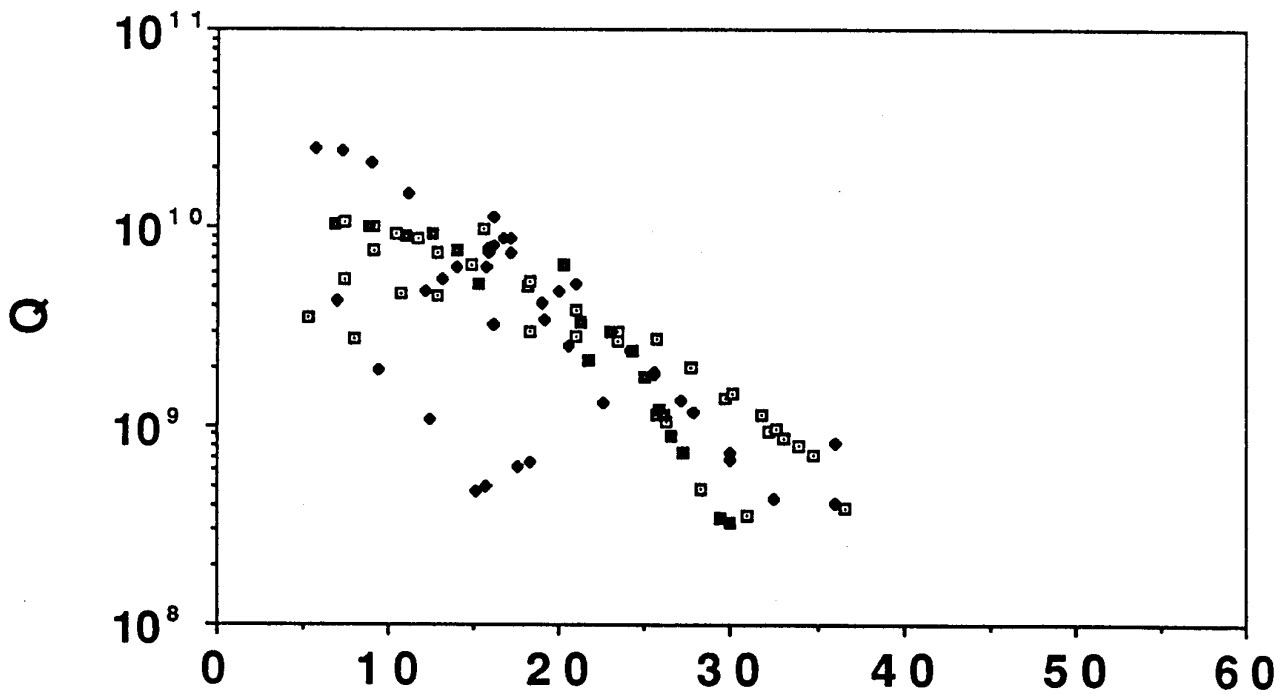
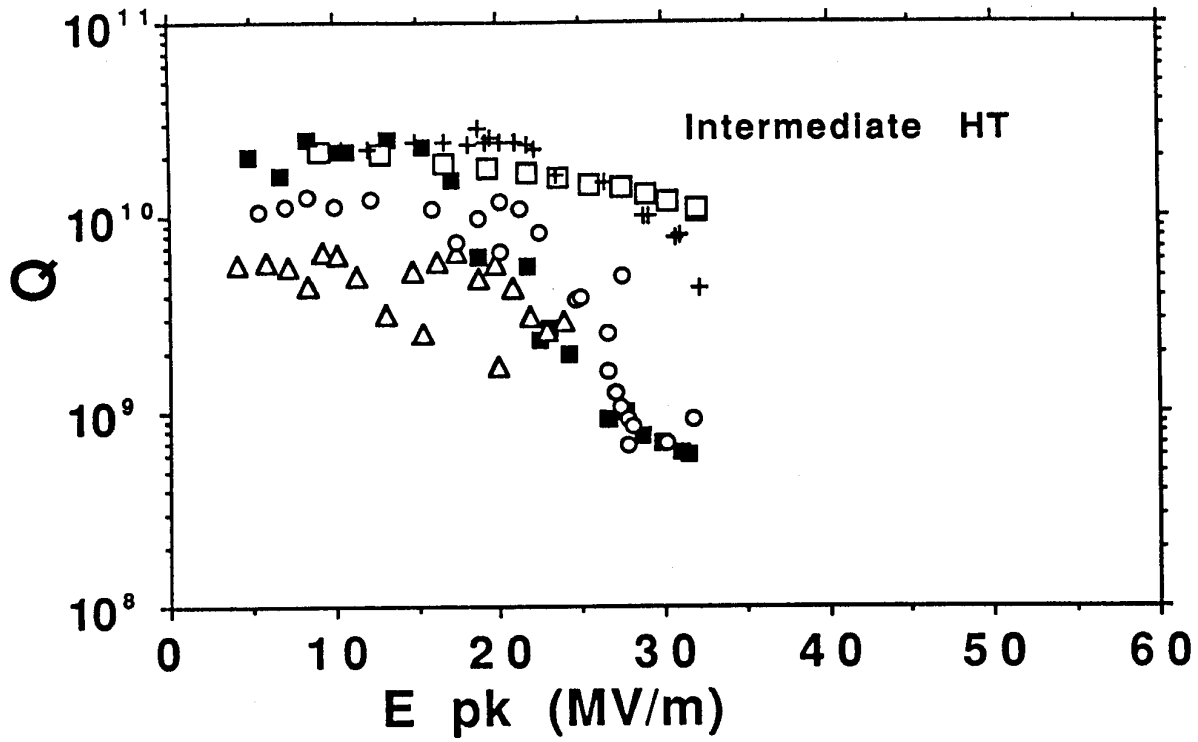


Fig. 11 Performance of intermediate heat treated cavities compared with chemically treated surface. All test results are for "virgin" surfaces which accounts for the noisy data.

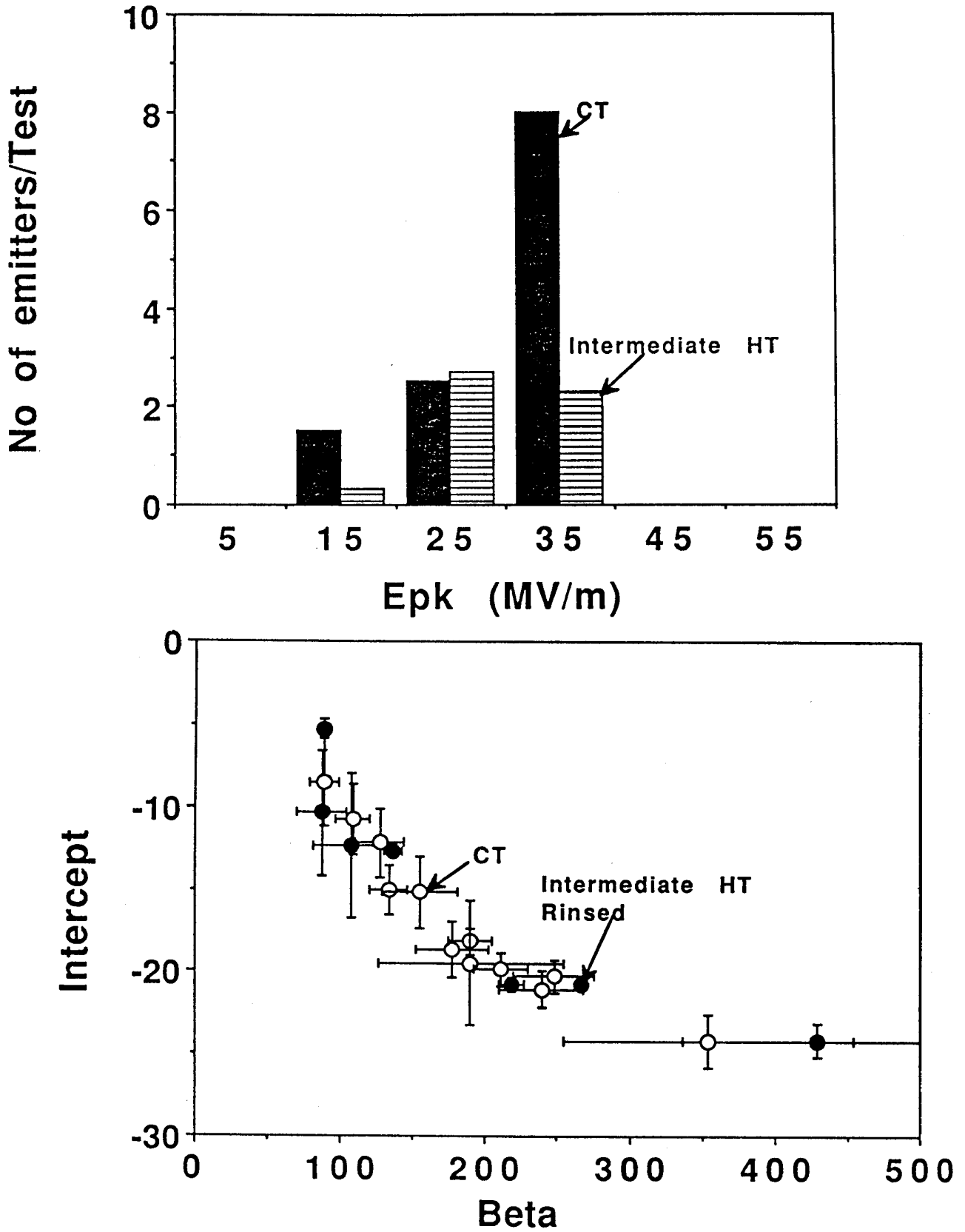


Fig. 12 Emitter density and emitter properties for intermediate heat treatment, compared to chemical treatment.

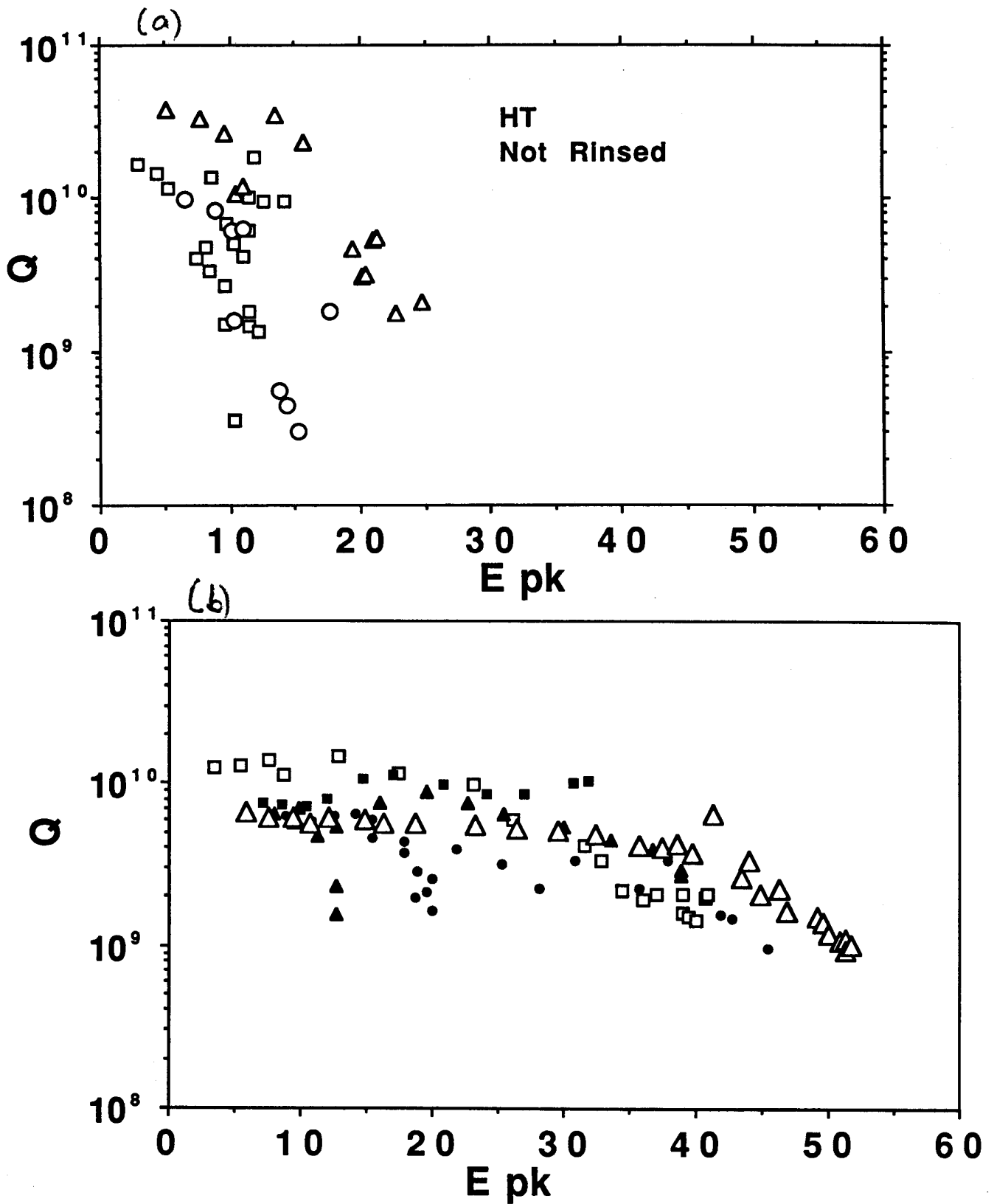


Fig. 13 Performance of intermediate heat treated surface that was not rinsed after removal of cavity from furnace. Performance for cavities heat treated at 1300 -1350 C is reproduced here for comparison. (b)

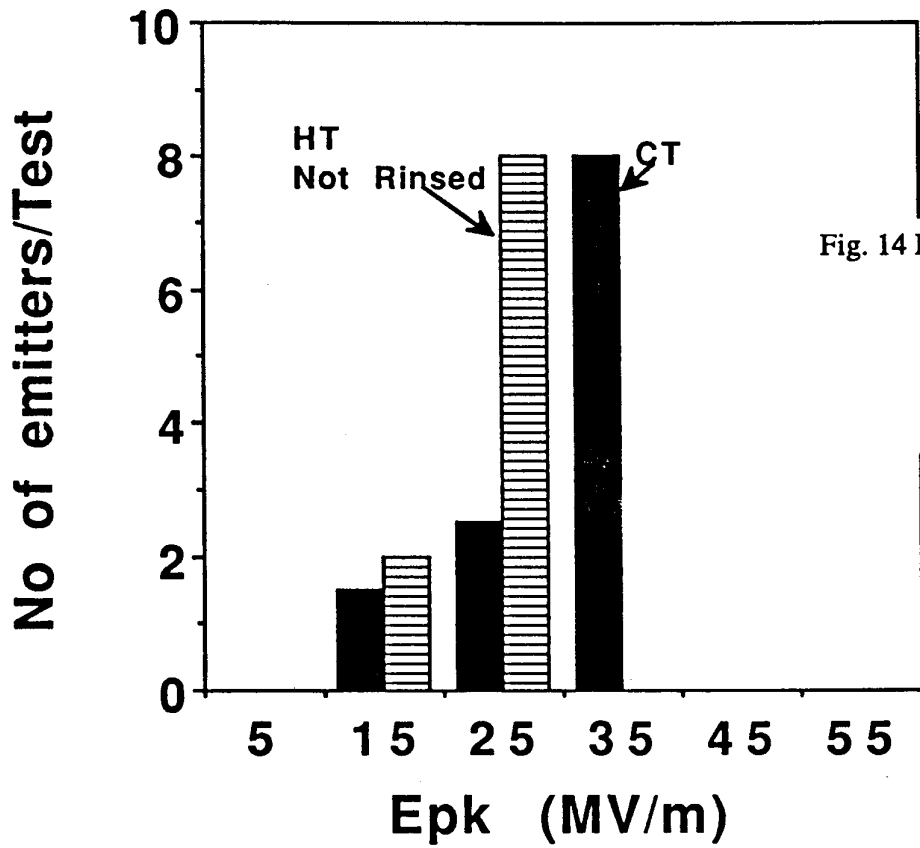
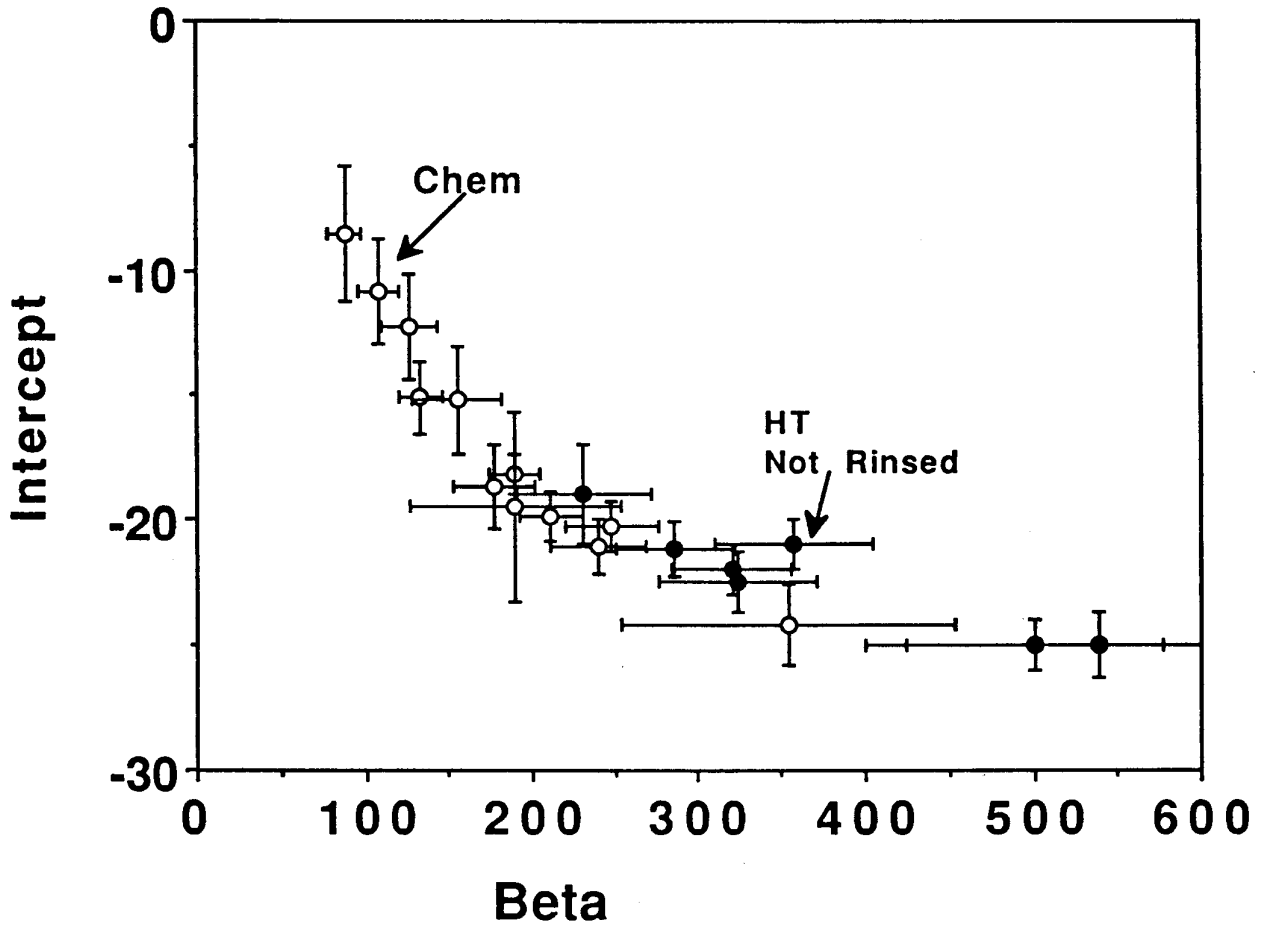


Fig. 14 Density and Fowler Nordheim properties of emitters detected on intermediate heat treated cavities tested without rinsing. A comparison to CT surfaces is given to show that rinsing is essential.



4.0 He Processing

The degree of improvement with He processing varies from case to case although as a general rule there is always some improvement. He processing was successful in levelling Q vs E curves to 30 MV/m in most HT cases, as shown in Figs. 15(a)-(d). As mentioned before, the 1300-1350°C HT cases were already substantially level with the virgin surfaces. It is encouraging that emitters present in intermediate HT cases (with or without rinsing) yielded to the remedy of He processing, suggesting that even intermediate heat temperatures did have some effect on the nature of emission sites. The least benefit from He processing was apparent in the CT cases. Significant drops in Q are observed even after He processing above 20 MV/m in all three CT cases previously discussed.

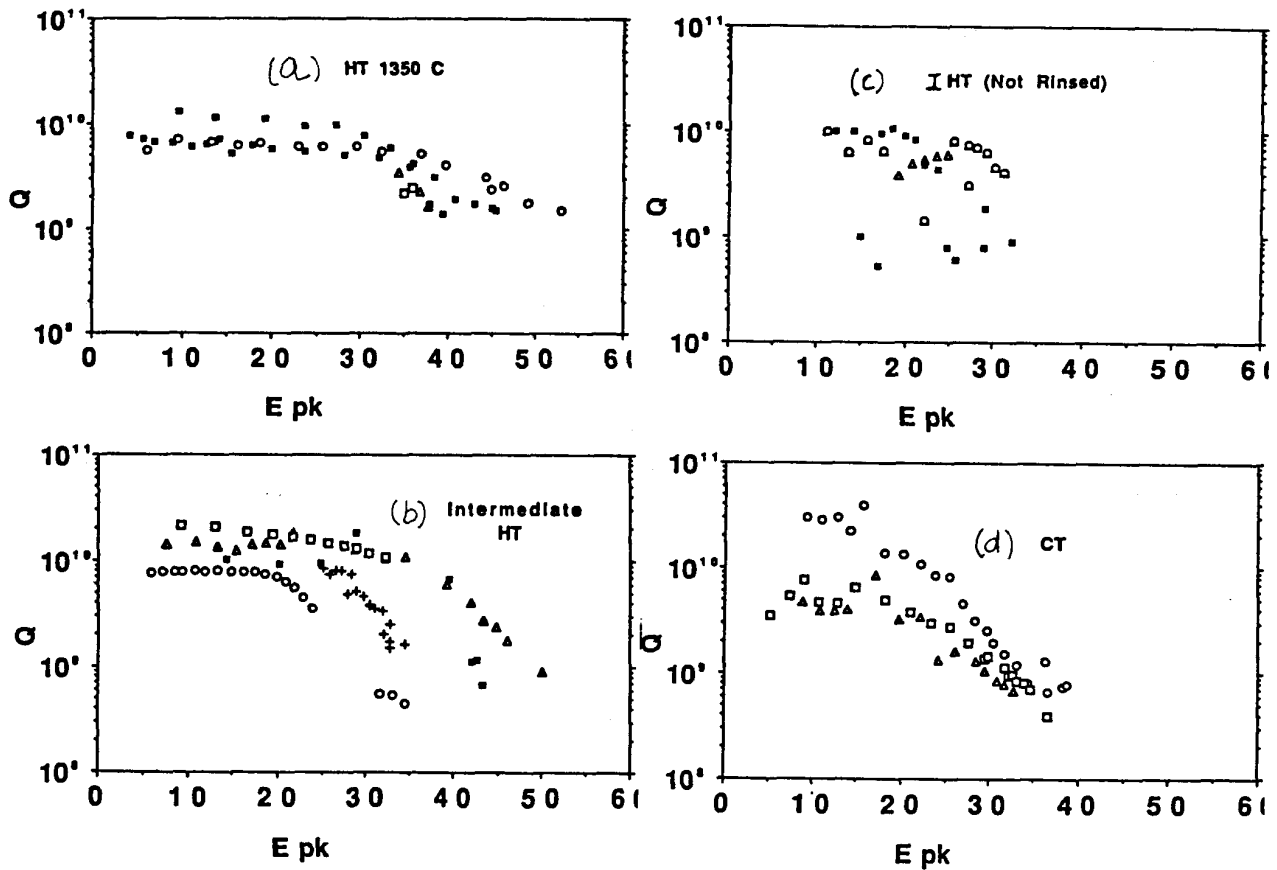


Fig. 15 Performance of four types of surfaces after He processing : (a) Heat treated at 1300 - 1350 C for long times (b) intermediate heat treatment (c) intermediate heat treatment without rinsing (d) chemical treatment.

Emitter density distributions after He processing are compared in Fig. 16 (a) - (d) with distributions presented earlier without He processing. One should focus the comparisons on the higher field data points as we have relatively little data at low fields after He (and prolonged RF) processing has been applied. Note that there are no significant changes in the distributions for the CT, highest-temperature HT, and intermediate-temperature HT cases. Only the non-rinsed intermediate-HT cases benefitted appreciably in reduction of emitter density after He processing.

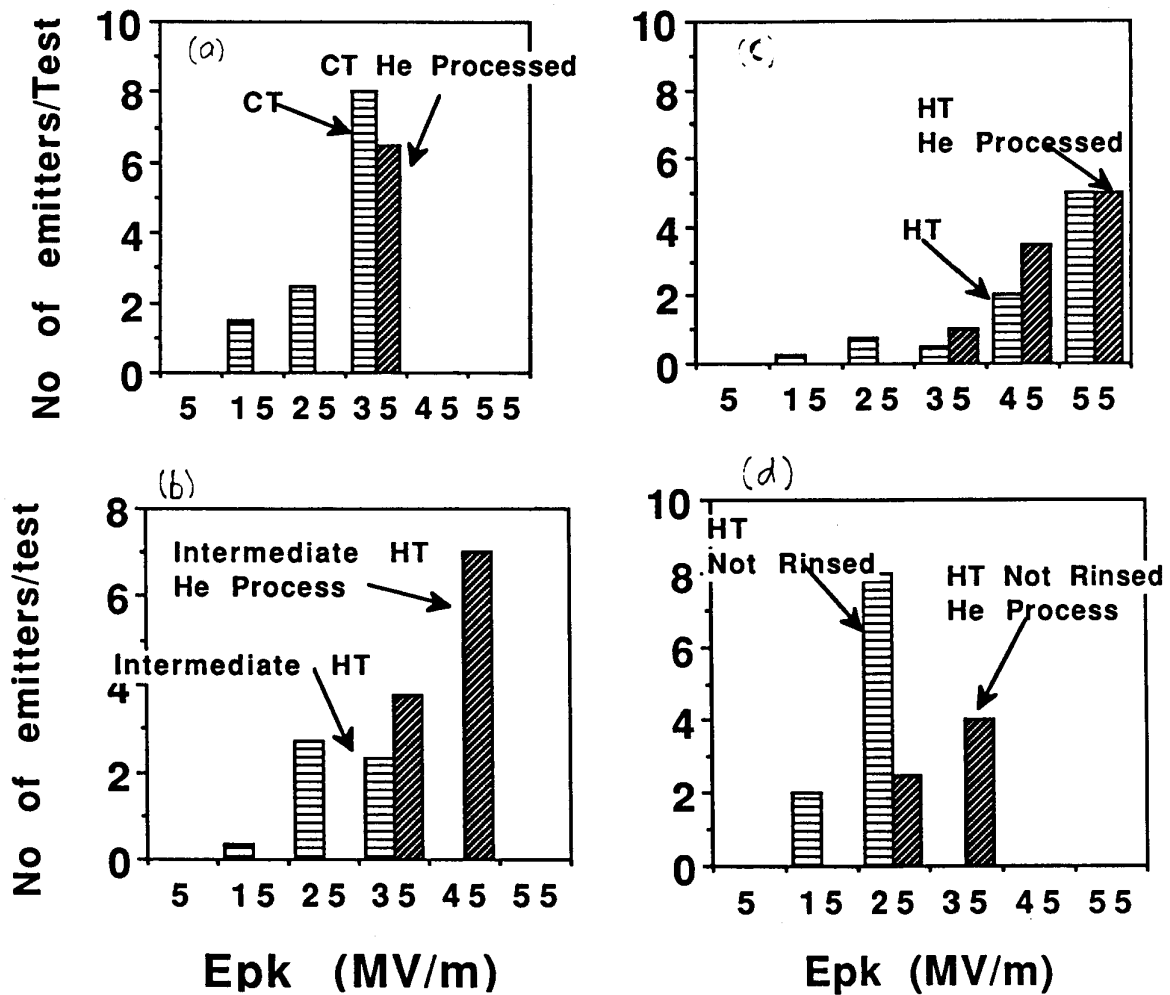


Fig. 16 Emitter densities before and after He processing for four different types of surfaces
 (a) chemical treatment (b) Intermediate heat treatment (c) heat treatment at 1350 C
 (d) intermediate heat treatment without rinsing.

Comparisons of the individual emitter properties before and after He processing is presented in Fig. 17(a)-(d). In the CT case there is virtually no change in the envelope. High β (>150) values are present even after He processing. In the highest HT case there is an elimination of β values >150 . Below $\beta = 150$ the envelopes overlap. The intermediate HT case shows a downward shift of the complete envelope after He processing, whereas the He processed emitter data on cases without rinsing after HT are too sparse to draw any firm conclusions.

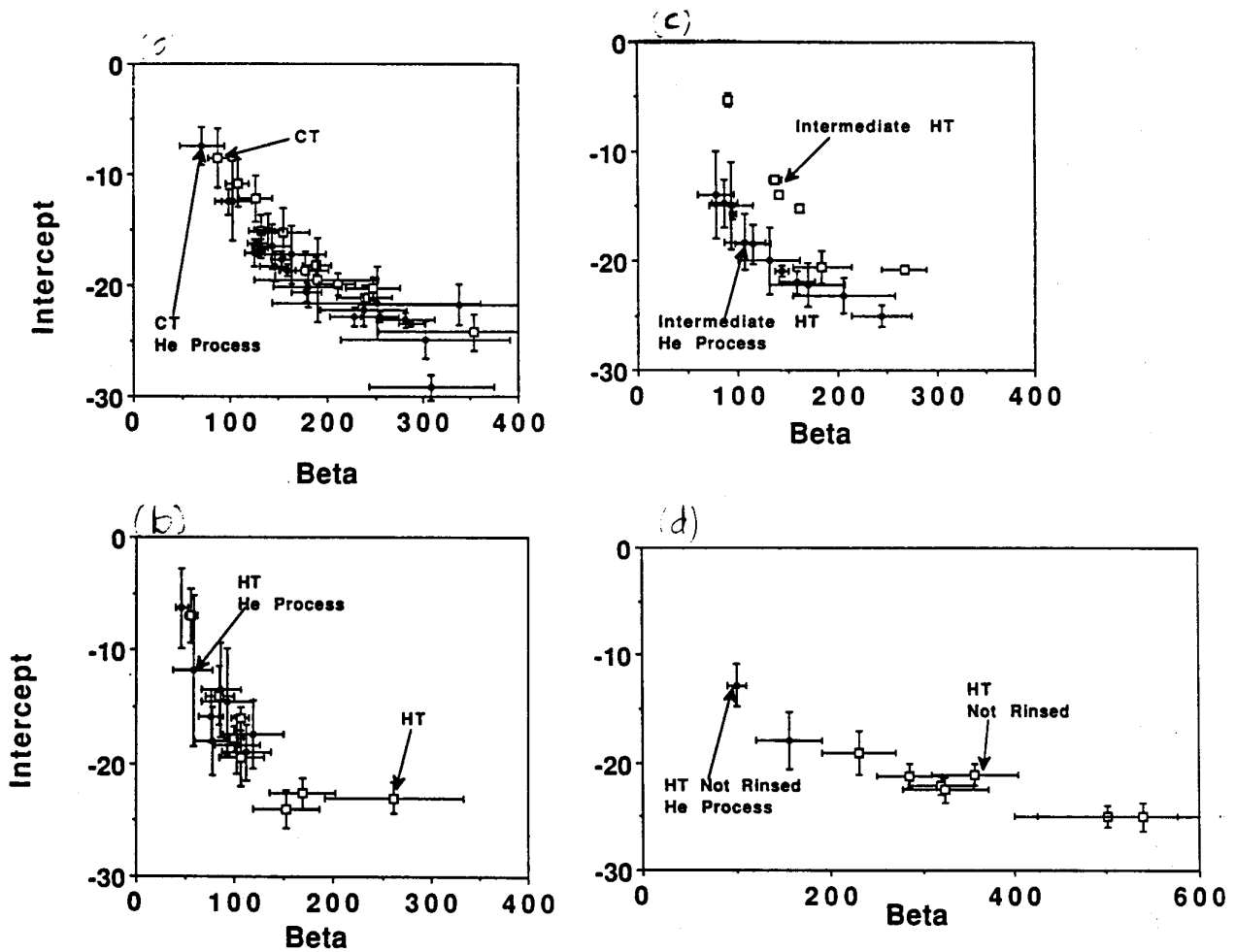


Fig. 17 Comparison of individual emitter properties before and after He processing for four different types of surfaces (a) chemical treatment (b) Heat treatment (c) intermediate heat treatment (d) intermediate heat treatment without rinsing.

The highest fields obtained in all heat treatment cases are displayed in the histogram of Fig. 18(a), along with a comparison with a large number of tests with chemical treatment alone. Results are shown without (a) and with (b) He processing. On the average He processing allows 20% higher field levels. In comparison heat treatment has a much more pronounced effect in improving field levels. The surface fields in 13 tests with HT was 40 MV/m as compared to the chemical treatment average of 25 MV/m.

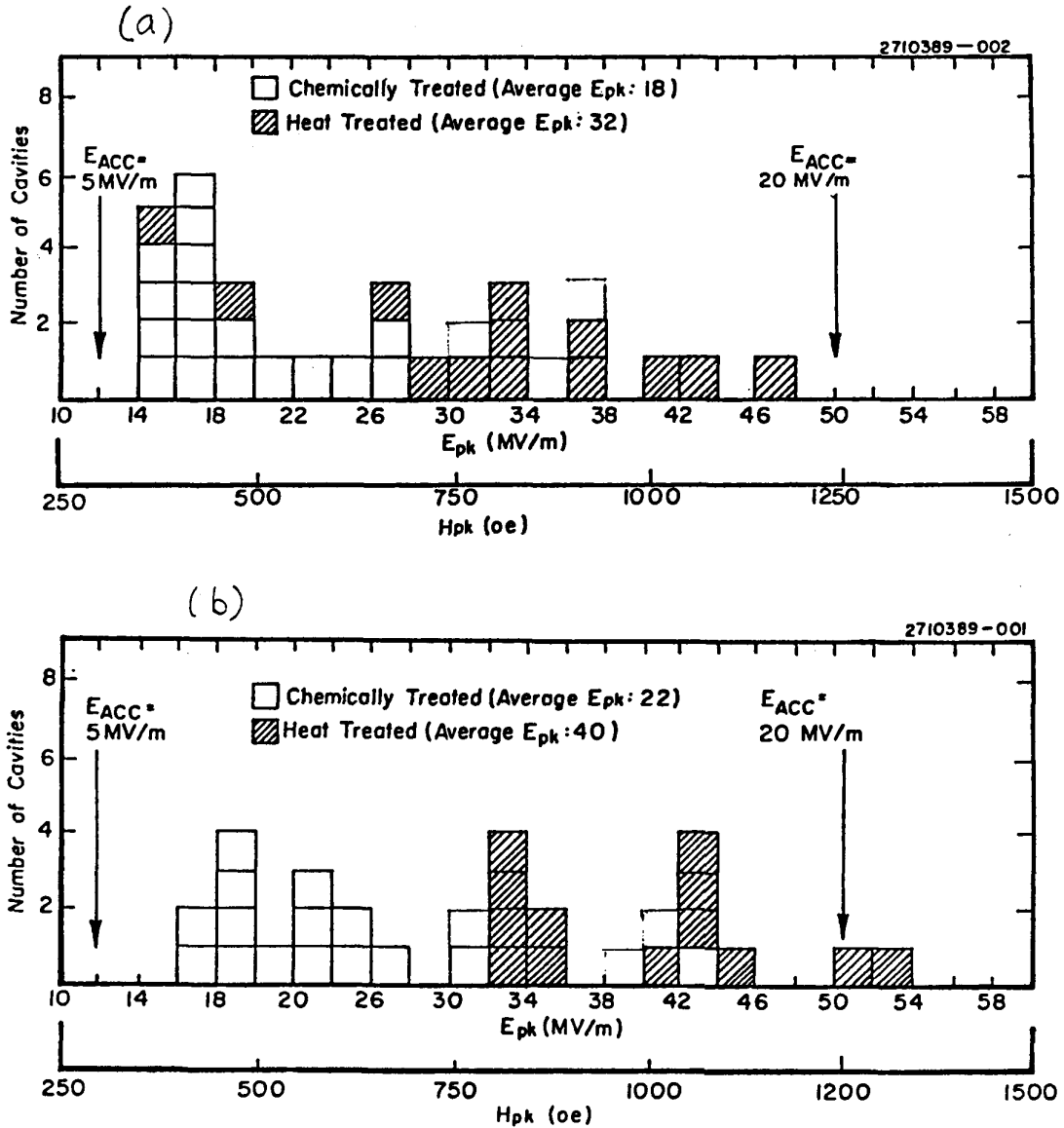


Fig. 18 Maximum fields reached (a) without and (b) with He processing.

5.0 Heat Treatment of 3-GHz Cavities

Very recently Wuppertal U. [17] has used a 1350°C heat treatment with Ti protection on a 1-cell 3-GHz Nb cavity. The cavity was rinsed with methanol after removal from the furnace and then RF tested. In the RF test no field emission was observed up to a peak surface field of 70 MV/m, a new record for this series of tests. Until this test the need to preserve a high RRR restricted most heat treatments to temperatures between 850°C-1200°C and periods to 1-4 hours. No rinsing was performed after the heat treatment, but care was taken to keep the cavities as dust-free as possible. A comparative histogram of highest fields reached after HT and CT is given in Fig. 19[8]. At this stage the statistical difference between HT and CT is not as apparent as with 1.5-GHz cavities, keeping in mind that only one test has been performed at 1350 C.

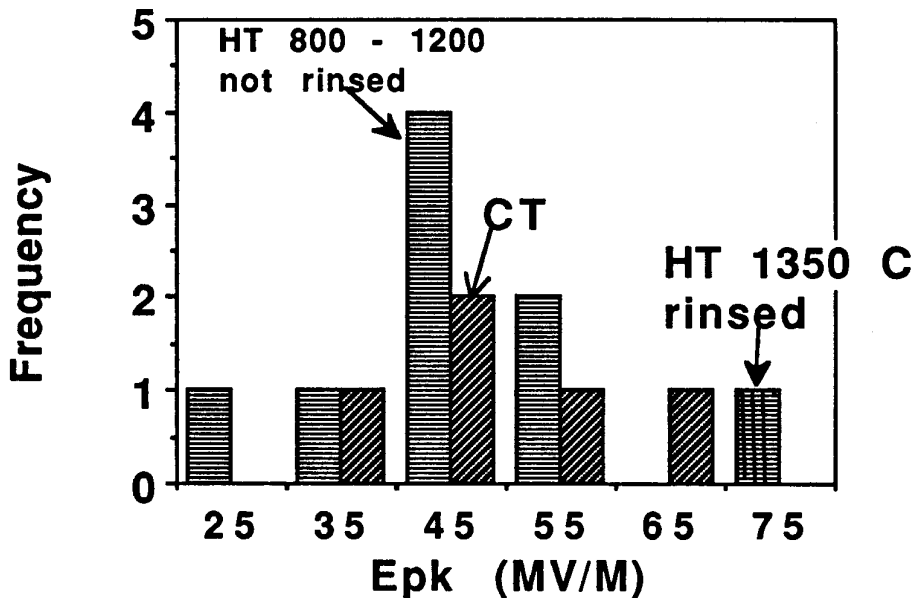


Fig. 19 Comparison of heat treated and chemically treated S-band 1-cell cavities tested at U. of Wuppertal. Heat treatments were mostly at 850 for 1 hour and not followed by rinsing. One heat treatment was at 1200 C for 4 hours, not rinsed. Very recently a 1350 C heat treatment with Ti protection followed by rinsing gave the best result.

6.0 General Inferences Concerning Emitter Properties.

Figs. 20(a) and (b) show the overall statistical distribution of intercept values and beta values obtained for over 100 emitters analyzed from the Cornell temperature maps. The intercept distribution is consistent with a gaussian but the β distribution is an exponential-like tail. We believe that the drop in β values below 100 is not real; it only reflects our inability to see these emitters at field levels accessible today. It is more plausible that an increasing number of low- β sites will continue to appear as higher- β emitters are eliminated. Fig. 20(c) resolves the total β distribution into separate components of the HT (highest temperature) and CT cases. Emitters that appear after He processing are included. (We do not attempt even finer resolution for the intermediate HT cases or for the non-rinsed cavities.) Although the shape of the distributions is the same, the HT distribution has a lower exponent than the CT. These distributions are remarkably similar to those obtained in DC field emission studies[12]. They also support the distributions hypothesized in statistical models [18,16,8] proposed earlier. Better distributions are thus available for new Monte Carlo simulations now in progress. Fig. 21 shows the distribution in βE_{pk} for all the emitters analyzed and separately for emitters in cavities prepared with HT and with CT. The distribution has a maximum at βE_{pk} of 4500. Earlier suggestions [19] were made that the most probable value of βE_{pk} is 5000. Data here is consistent with this suggestion for emitters belonging to either the HT or the CT class.

This behavior is particularly interesting in view of the fact that the E_{pk} values for the two cases were different by $\sim 50\%$. For the HT case most of the E_{pk} values were around 45 MV/m and for the CT case they were around 30 MV/m. We observe that emissive areas appear to be randomly distributed, i.e. the distribution of $\text{Log}(\text{emissive areas cm}^2)$ appears to be random around -9, [$\text{log}(\text{intercept}) \sim -17.5$]. It is possible to interpret the most probable measured $\beta E_{pk}=4500$ as indicative of a limit of the ability of Nb cavities to withstand field emitted currents far above that given by $\beta E_{pk} = 4500$.

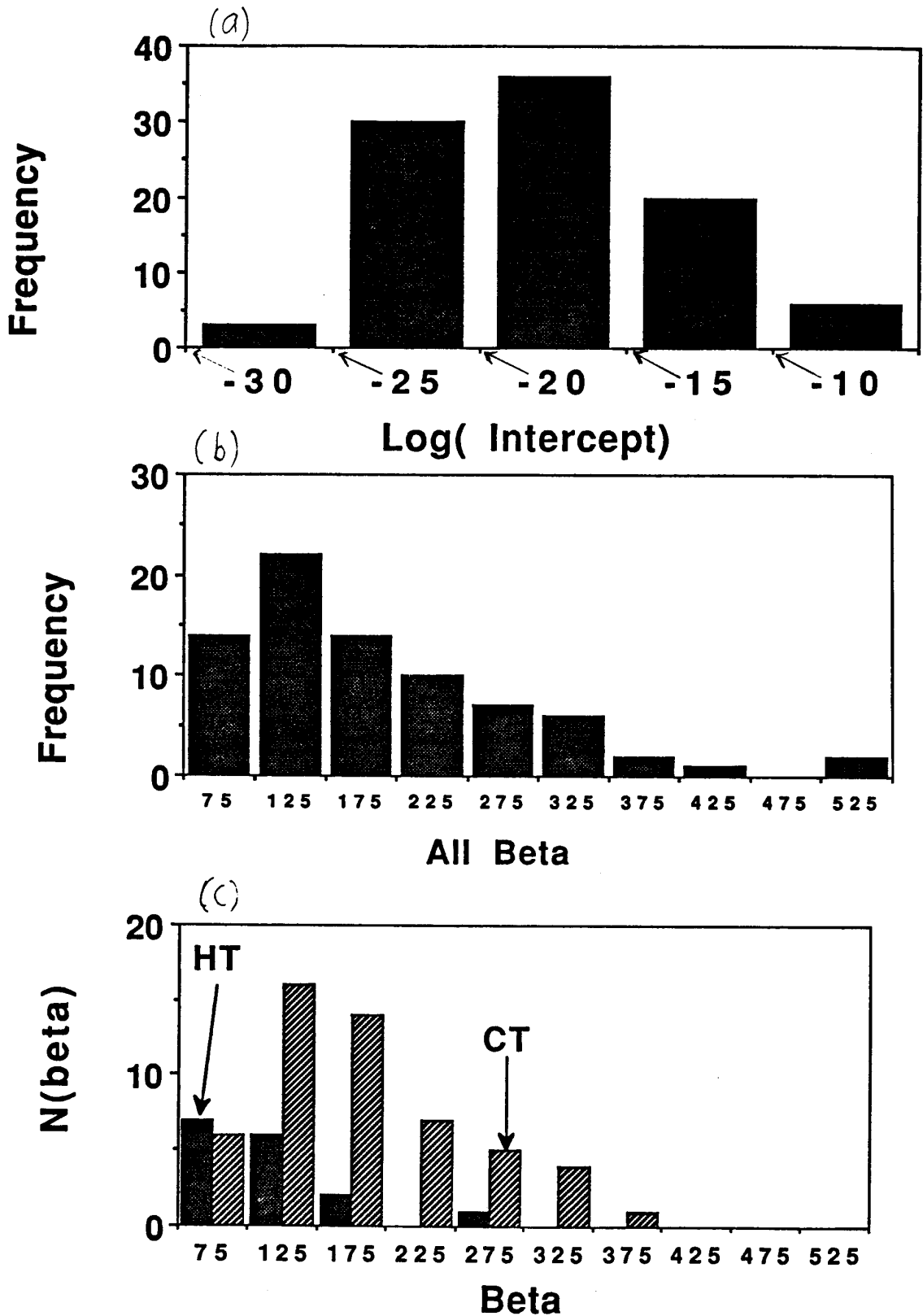


Fig. 20 Overall properties of more than 100 emitters studied. Note that in (a) the distribution of log (intercept), ie. log (emissive area) is random but that in (b) distribution of beta increases sharply with decreasing beta values. To convert intercept to emissive area use : $\log(\text{area-cm}^2) = -1.65 + 0.44 \cdot \log(\text{intercept})$ obtained from simulated temperature maps. Part (c) gives separate beta distributions for heat treated and chemically treated surfaces.

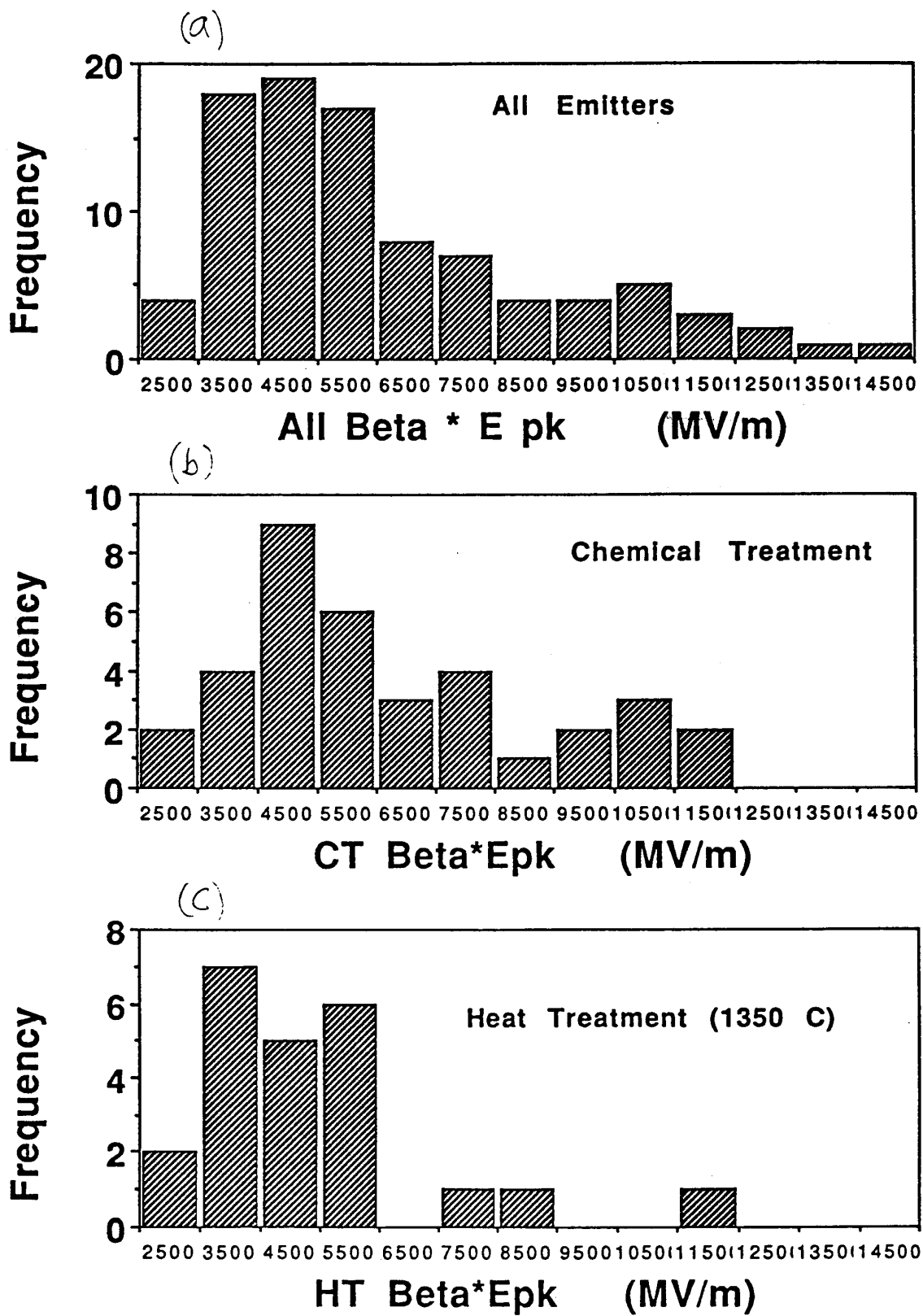


Fig. 21 Distribution of βE_{pk} for (a) all emitters (b) emitters from chemical treated surfaces and (c) emitters from HT surfaces. Note that the maximum is nearly the same in all three cases.

7.0 Influence of condensed gases.

One phenomenon suggesting the importance of condensed gases to field emission is the change in the emission landscape often observed after warming a cavity to room temperature and then cooling down without physically disturbing the test set-up[20]. In our experience, some changes in the Q vs E behavior are observed near the highest field level, but RF processing and occasionally He processing are always sufficient to restore the performance levels after RT cycling. Two examples were given in [20] at 38 MV/m. Fig. 22 gives another example at ~50 MV/m. Incidentally these maps were taken at and near our record fields. To the best of our knowledge these are the first maps at these high field levels. Emission spots are shaded for visual clarity after they were positively identified as emitters.

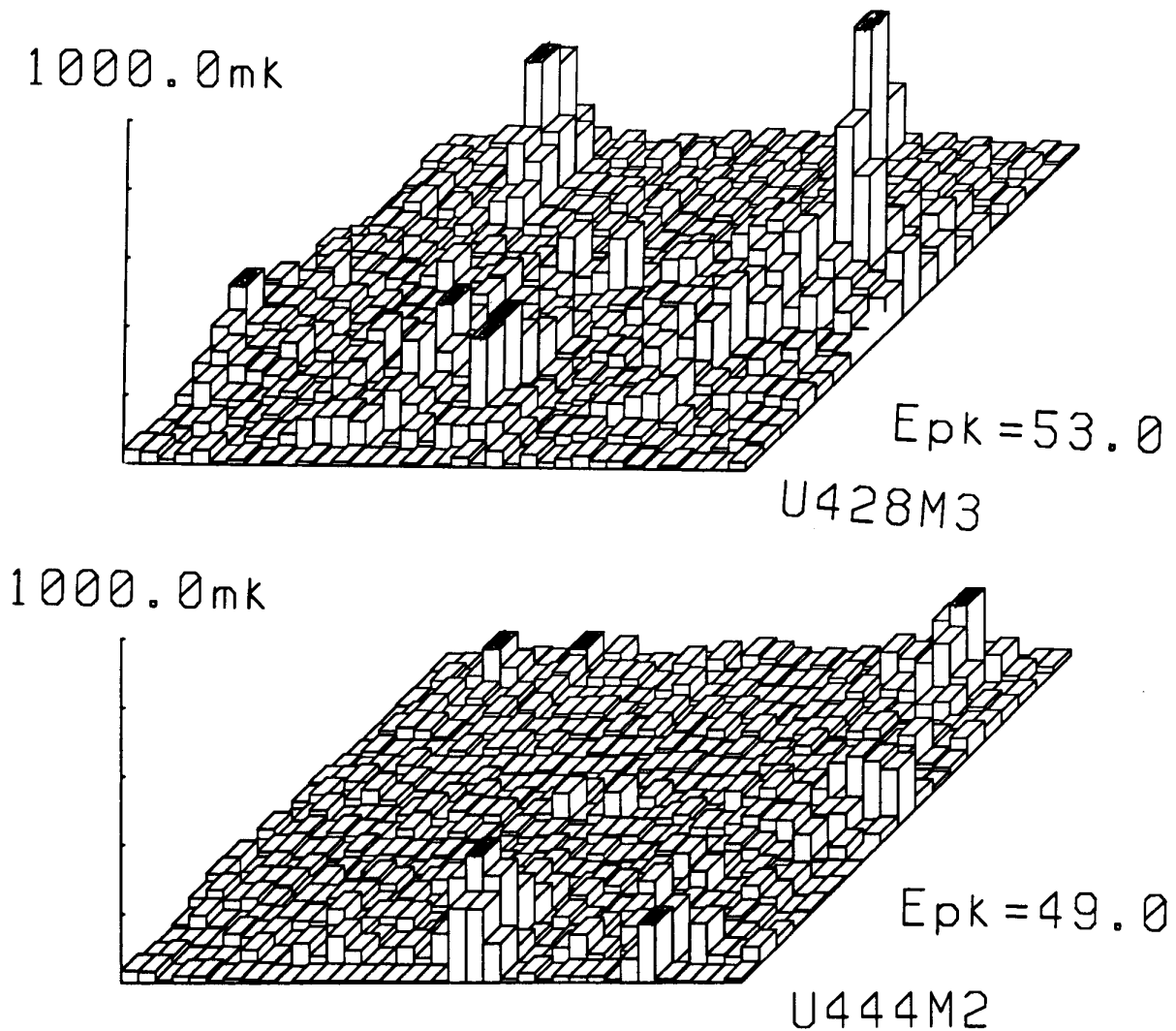


Fig. 22 Change in emission landscape from cycling a cavity to room temperature. Current interpretation is that there are a large number of dormant sites in each test that can be activated by movement of condensed gases during room temperature cycling.

Though one can imagine other mechanisms to explain these effects, the most likely seems to involve condensed gases. A site caused to emit more strongly by an overlying layer of gas might be extinguished by the removal of the gas in warming up under vacuum; as the cavity cools again, residual gases may occasionally re-condense on a potential emission site, thereby activating it.

A second observation suggesting the importance of condensed gases comes from our experience with He processing. Occasionally admission of He into a cold cavity for processing is observed to activate emission. Fig. 23 shows three maps from one cavity taken before RT cycling, after RT cycling and after admission of He. After RT cycling map (b) shows that previously dominant emitters in map a are now quiet. On readmission of He we note in map (c) that one of the old emitters visible in map (b) is now re-activated. This behavior can be explained by contaminants present in the He that recondense on an emission site which has been deactivated by RF cycling.

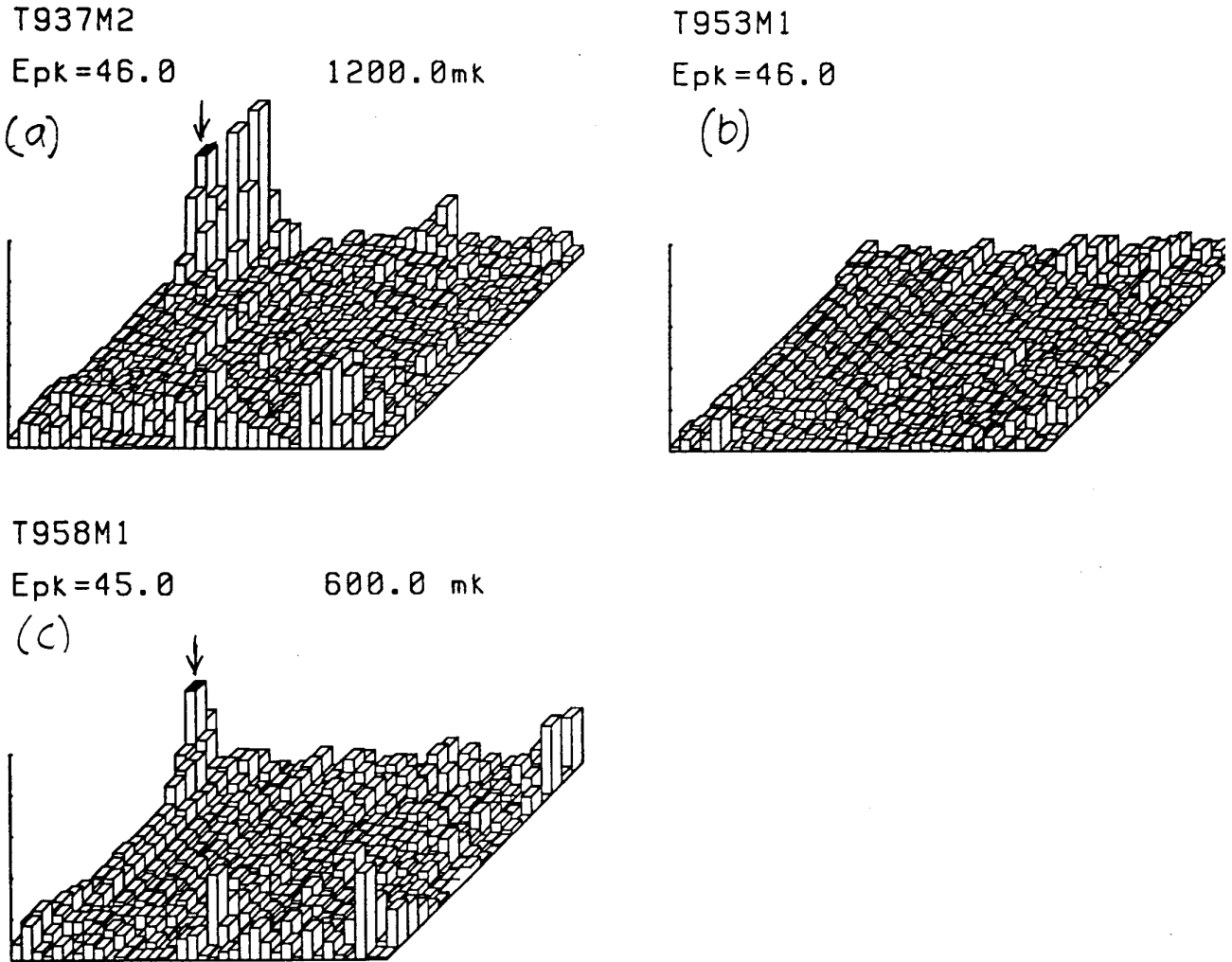


Fig.23. Activation of a dormant site by admission of He gas. Active site in (a) marked by arrow becomes dormant after room temperature cycling (b) Admission of He gas (c) re-activates dormant site.

Motivated by these observations, we have carried out more direct experiments in which a cold cavity was intentionally exposed to a large dose of high purity oxygen gas (Fig. 24(a)-(d)). During gas admission a constant pressure of 100 mtorr was maintained at the room temperature end of the cavity vacuum pipe. We suspect that most of the gas condensed along the cold pipe wall before even reaching the cavity, but a small fraction could condense on the cavity wall. Fig. 24(a) (26 MV/m) shows the emission landscape before gas exposure, and (b) (16 MV/m) shows the appearance of a new strong emitter a few minutes after start of gas admission. Subsequently the cavity was brought to room temperature without any mechanical disturbance and then pumped out. On re-cooling, maps taken at the same field level (16 MV/m) showed that the strong, oxygen activated emitter was gone and it was possible to reach a higher field of 22 MV/m, at which stage map (c) was taken. The disappearance showed that the incident of emission increase with gas flow could not have been caused by "dust" particle introduction. Oxygen was again admitted into the cavity. The same strong emitter re-appeared promptly as seen in map (d), and the field again fell to 18 MV/m. In the second exposure we reduced the oxygen flow

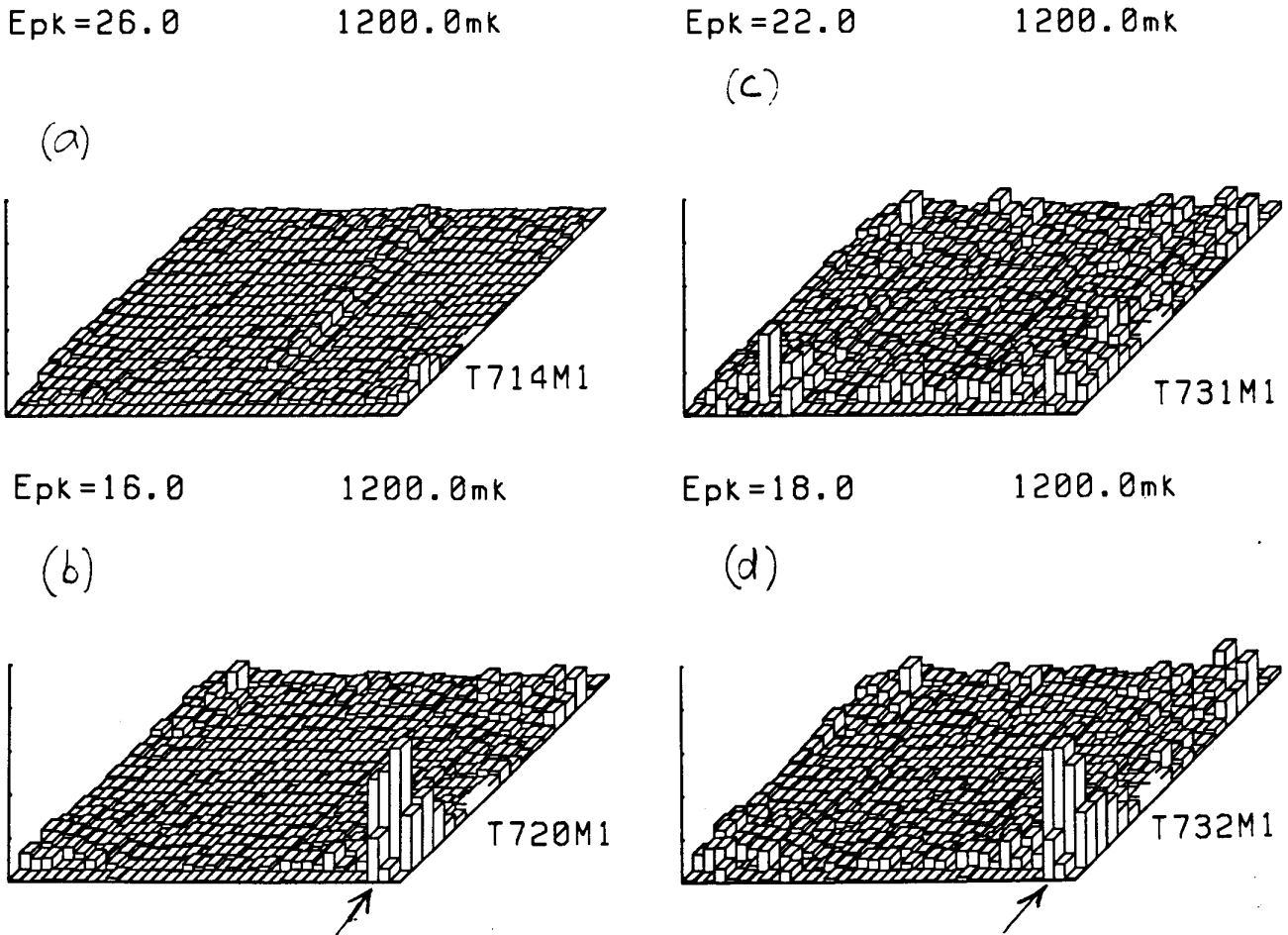


Fig. 24 Influence of deliberate oxygen gas exposure. Starting with an emission free surface (a), strong emission is induced by dose of oxygen gas (b). Emission at this site is eliminated upon cycling to room temperature (c), but reactivated by second exposure to oxygen gas (d).

substantially to avoid the formation of "snow". Only one charge (100 cc x 100 mTorr) was admitted. From these experiments the explanation that emitters are activated by condensed gases is most plausible. We note that subsequent He processing for a few minutes suppressed emission at this site and the field of 23 MV/m was recovered. We thereby also confirm that one of the mechanisms whereby He processing is beneficial is in removing condensed gases.

Although evidence of changes in FE due to condensed gases in RF cavities has also been presented by others, to the best of our knowledge this study provides the first direct evidence of their effects. At CERN, a cold cavity equipped with an accelerator vacuum beam tube was exposed to the equivalent of 5 monolayers of a typical accelerator residual gas atmosphere ($H_2:H_2O:CO:CO_2 = 69\%:17\%:8\%:6\%$). The onset of FE electron loading remained unchanged at 10 MV/m (surface field) for the first monolayer of exposure. After that the field dropped to 7 MV/m, confirming the influence of condensed gases[16].

Copper cavities which have been processed with very high power (50 MW, 1 μ s) are reported to need additional processing of a few minutes after several days of exposure to 10^{-7} to 10^{-8} torr[21]. In comparison, immediately after processing is complete, the same cavities can be taken from the low-field to the high-field state instantaneously. Deliberate exposure to CO gas increases FE current and requires 15-30 minutes of additional processing to recover. As a baseline we note that for a virgin copper surface the processing time is usually between 3 to 14 hours to reach fields of 200-500 MV/m.

A older theoretical study has shown that it is possible for a resonant tunnelling process through a thin overlying insulating layer on a field-emitting pure metal surface to increase emission[22]. While the basic emission process present in SRF cavities must be more complex, a similar resonant tunneling process can presumably also enhance the emission in this case. In light of the role of condensed gases in aggravating emission, it will be important to explore the possible benefits of cooling cavities in a better vacuum, as well as to attempt better outgassing of the RF surface before cool down.

8.0 Sources of emitters.

A superconducting cavity surface is exposed to various media in the course of its preparation: chemicals, water, methanol and class-100 air. In a recent series of experiments we tried to evaluate the relative importance to FE of each of these agents. We were on the look-out for substantial increases in FE accompanied by enhanced density of emission sites. By these tests we showed that clean water exposure is more harmful than clean methanol exposure, and that chemical treatment is the most harmful of the three. A separate paper on these experiments is presented at this workshop[23]. Here we summarize the main results.

Our strategy was to prepare baseline reference surfaces with as high a field as possible ($E_{pk}=30-50$ MV/m) and to archive their FE behavior in RF fields with Q vs E curves and temperature maps. To produce these high-field reference states, we used heat treatment followed by He processing. Subsequently we "exposed" the cavity surface and re-tested the RF behavior comparing Q vs E curves and maps before and after exposure. For each exposure test we prepared a new reference baseline RF behavior prior to the exposure so that degradation effects would not propagate. Each agent was evaluated with at least two exposures.

Clean Air.

We chose to first study clean air, as this is the final agent in contact with every RF surface before evacuation. Very little change was observed in Q vs E behavior or in the landscape of emission sites at 30 MV/m showing that class-100 clean air is not a copious source of emission sites. Other workers have also shown that exposure to clean laboratory air does not change the FE activity dramatically. [16,12].

Clean Methanol.

Starting with a baseline RF surface that could reach 40 MV/m, we exposed this surface to clean methanol, followed by class-100 clean air. (It was necessary to first expose the surface to clean N_2 to let up the vacuum but it is plausible to expect that the subsequent rinse and air contact will play the dominant exposure role.) After exposure, we observed no significant deterioration below 30 MV/m. At 34 MV/m emission was stronger and dominated by a single site. After He processing this site disappeared and it was possible reach 42 MV/m with about the same emitter density as the reference surface. A second baseline reference followed by a methanol exposure test showed no deterioration below 45 MV/m. These results lend confidence to rinsing cavities with methanol as a routine cleansing procedure, for example after removal of a cavity from the furnace.

Clean Water.

Next we evaluated the effects of exposure to clean water (resistivity 18 M Ω -cm, filtered with 0.2 μ m filters), followed by drying in class-100 air. Significant increases in emission loading was observable above 25 MV/m and two strong sites were present at 38 MV/m as compared to none for the reference, reducing the Q by an order of magnitude. This was the strongest emission increase from exposure observed yet. He processing was successful in eliminating the sites and in restoring the Q at 38 MV/m to the reference level. Here thermal breakdown was encountered, which was most likely from a defect introduced by the water rinse. A second water exposure was performed on a baseline reference surface that reached 39 MV/m. Again substantially increased FE was observed at 15, 25 and 39 MV/m, as compared to the reference. Once again He processing eliminated the enhanced emission and restored the baseline performance all the way up to 39 MV/m. Both water exposure tests influenced emission more strongly than both methanol exposures, indicating that water introduces more sites than methanol. It is encouraging that all these sites could be removed by He processing.

Chemistry.

Next we tested chemical treatments on separate surfaces which could reach 53 MV/m and 33 MV/m. Naturally the chemical treatments were followed by standard water, peroxide, and final methanol rinses, and drying in class-100 air (see Table 2). We already know how much deterioration to expect from these subsequent agents (except peroxide), so that the results of the experiments can easily be interpreted. In both chemical treatment cases we observed substantially enhanced FE behavior above 25 MV/m (an order of magnitude drop in Q). Indeed, the performance of these chemically treated cavities was indistinguishable from that of chemically treated virgin cavities--there is no memory of the benefits of heat treatment. He processing helped somewhat but did not recover the reference behavior in either case, unlike the cases of water and methanol rinses.

One possible interpretation of the large increase in emission is that chemical residues are a dominant emission source. Another is that new inclusions in the Nb material are exposed during each chemical treatment and these are potent emission sources that require more drastic remedies, such as (further) heat treatment.

Pursuing the first possibility we tried to improve rinsing. Starting with a reference cavity that reached 44 MV/m, we chemically treated it and followed it by extending our standard water rinsing of 2 hours (see Table 2) to 8 hours. During most of the long rinse we connected the cavity in the closed polishing loop of our clean water system. As a result the cavity was continuously replenished with clean water. We estimate a total of $\sim 10^4$ volume

changes. Ultrasound agitation was incorporated during the long rinse and the water temperature was elevated to 50°C, following improvements at 20 MV/m observed by the KEK rinsing procedure[6]. All these measures were added to better dissolve acid residues or precipitates that cling to the Nb surface. Once again, the RF test showed heavy FE as with other CT cases. He processing was no more effective than other CT cases. We intend to repeat this test, but the results are not very encouraging for reaching fields above 30 MV/m.

9.0 Lessons to be Learned from Copper Cavities and High Power Processing

In the last few years extensive tests have been conducted on copper RF cavities in the frequency range from 3-11 GHz[21]. These cavities are processed with very high peak power klystrons, e.g., at 2.9 GHz, 50 MW with RF pulse length of 2.5 μ s at a 60-Hz repetition rate. Using these techniques peak surface field between 200-600 MV/m have been reached after processing times of 3-14 hours. FN plots of the emission current after processing yield β values of ~ 60 . Unlike Nb cavities, processing of Cu cavities under these conditions takes place predominantly via RF sparking. During such a spark (or RF breakdown) the emitted current is observed to increase by a factor of 20-30 and the vacuum degrades from 10^{-8} to 10^{-7} torr. It is believed that the local FE current density approaches 10^9 A/cm², which is considered sufficient to reach melting conditions near the emissive spot. Current densities of this size are consistent with the several 10's of MW of RF power required to bring about explosive processing in Cu cavities. Subsequent visual inspection of high-field regions show numerous crater-like holes, several 10's of μ m in diameter and molten beads of copper in low E field regions.

By contrast, in a superconducting Nb 1-cell, 1.5-GHz cavity operating at 40 MV/m, an emitter with $\beta=100$ and an emissive area of 10^{-8} cm² will produce average emission current of 1 μ A which will deposit ~ 1 W of power on the wall. Such an emitter will produce a 1 K peak temperature signal in a superfluid thermometer such as those used in our diagnostic system. This is typical of a strong emitter seen in a test of a 1.5-GHz HT cavity. However the emission current density of this Nb cavity emitter example is only 100 A/cm², seven orders of magnitude below the explosive processing regime.

An interesting question here is whether there is a happy medium between these two regimes. On the one hand, in cw sc cavities we put very low powers (1-10W) into the field emitters and see minimal RF processing, ignoring He processing which presumably works by other mechanisms. In the other extreme, copper cavities use 10^7 W (μ s pulsed) and successfully process away emitters. However, the resulting craters or beads which may not be harmful for μ s operation of copper cavities are very undesirable for long-pulse (ms) to cw

operation of Nb cavities. Such features will initiate thermal breakdown. Therefore explosive processing is unsuitable for Nb cavities.

Some exploration of the region in between was carried out in the high power pulsed processing work on Nb cavities by Campisi et al[24]. With 1-2.5 μ s pulses of 1-2 MW peak power, it was possible to reach surface fields of 55 to 70 MV/m repeatedly in several cavities, without special care in Nb surface preparation. Low-power long-pulse tests on the same cavities reached 6-25 MV/m. The benefits of pulse processing for Nb cavities were clearly observed. However because of the fixed input power coupling system, it was not possible to determine whether the FE was permanently processed as is desirable for later long pulse or cw operation. It is in the applications that require long pulses or continuous voltages that sc cavities offer key advantages. Therefore it will be important to establish whether the benefits of high power processing extend to long pulse operation. Upto 2 kwatts of pulsed power is used by Argonne to process low β Nb structures.

At Cornell, we have begun a program to investigate RF processing with intermediate power levels (up to 200 KW). A separate paper is presented at this workshop giving the status of this work[25]. Our goal is to determine whether this technique can produce permanent improvements in FE behavior. Even if high fields can be reached for pulse lengths of 100 μ s they would be useful for operation of sc cavities in a future TeV linear collider. Accordingly we have chosen the pulse length as variable up to 2 ms and the external Q of the high power input coupler as variable from 10^5 to 10^{10} . First tests with a 1-cell 3-GHz Nb cavity have been performed, with encouraging results. In the first test, FE was observed to drop the cavity Q from 10^9 to 2×10^8 at 18 MV/m (~ 10 W of FE power). A few minutes of cw RF processing did not reduce the emission. No He processing was tried as we wanted to retain the FE behavior to evaluate pulsed high power processing. Subsequently 200 pulses of 50 KW and 100 μ s duration were delivered at a Q_{ext} of 10^6 , to maximize the power transfer efficiency. After processing, the coupling was restored to Q_{ext} of 10^9 and the low power cw source re-connected. The emission was found to be largely suppressed and a cw field of 20 MV/m was reached at a Q of 10^9 . Unfortunately thermal breakdown occurred at this field, the origin of which is not known. An important observation was that during pulsed processing the output coupler indicated that the cavity field reached 34 MV/m, which is well above the cw breakdown field. We believe this is consistent with the thermal time constant for defect growth of 1ms, observed in the past. Since the RF is shut off after 100 μ s there was not enough time for this defect to initiate breakdown.

10.0 New Results from DC Field Emission Studies.

At the U. of Geneva, a scanning tunnelling microscope (STM) has been added to the DC field emission study facility[26]. This facility has in the past yielded very useful results, improving our understanding of FE together with showing that heat treatment is an effective tool in reducing the density of emission sites on Nb surfaces and thus an effective remedy against FE. Plans with the STM are to eventually study FE sites with higher resolution than previously possible. This will help improve our basic understanding of the FE process. STM scans on an area of Nb ($16\mu\text{m} \times 16\mu\text{m}$), chosen to be free of any large emission sites, showed about half a dozen weak sites with enhanced emission corresponding to β values between 1.6 and 10 and emissive areas between 10^{-16} to 10^{-17} m^2 . Both the β 's and emissive areas of these sites are far below the range of emitters studied earlier ($\beta=50-300$, $S = 10^{-7}$ to 10^{-16} m^2). The total current was kept at 0.1 nA, as compared to earlier DC FE studies where currents of 40 nA were drawn.

New FE studies were also conducted on Al surfaces, which were found to be more emissive than Nb surfaces. Most sites were found to be particles of Ta and stainless steel covered by a film of Al. It is possible that these particles were embedded during the mechanical polishing stage of surface preparation.

At the U. of Aston, new gas conditioning studies on DC FE from Cu surfaces have been carried out[27]. Conditioning with He, Ar, O_2 , N_2 are all found effective, but at different gap voltages. H_2 conditioning is only slightly effective. With a typical gap separation of $5 \times 10^{-4} \text{ m}$ it was found that He conditioning at 5-10 kV reduces FE current by one order of magnitude. Above these voltages the conditioning effectiveness drops to zero. However Ar conditioning was found to be effective between 10 and 15 kV, O_2 conditioning between 12 and 20 kV and N_2 conditioning between 17 and 22 kV. The improvement with conditioning was substantially reversed by heating at 250°C for 2 hours.

Traditionally He processing has been interpreted as removal of FE-enhancing adsorbates in short time intervals, followed by sputtering of the bulk emitter over longer periods of time. The new conditioning results suggest a different model in which high-energy gas ions are implanted into an emitter, altering the solid state properties of the emitter and changing the I-V characteristics of the device. Different gas species require different gap voltages to penetrate to the effective zone. At 250°C the implanted ions diffuse away from this region.

11.0 Conclusions

At each SRF workshop the trend of increased field level with smaller area cavities is revisited, attributed to the decreased probability of emitters and defects. This trend is still obeyed, but there is also a continual drift upward in achievable field levels, as the purity

(RRR) of Nb cavities edges upward to provide stability against thermal breakdown, and as new techniques are applied to produce cleaner, emission-free surfaces. Peak surface electric fields in .35 to 1.5 GHz cavities have increased three fold in the decade since the first SRF workshop. New records have been reached at 1.5 and 3 GHz. Gains in 0.35-0.5 GHz cavities and structures are attributed to cleaner surfaces through improved rinsing techniques, bringing performance to 20 MV/m before FE loading becomes severe. Gains in high frequency cavities are based on high temperature treatment. Field emission still dominates above 40 MV/m, although RRR limitations are frequently apparent. The need for RRR above 500 will soon become paramount as surface magnetic fields above 1000 Oe progress from frequent to routine. It has been demonstrated that there is nothing intrinsic to a Nb surface that will in the future prevent the attainment of electric fields above 100 MV/m.

Benefits of high temperature treatment established in DC field emission tests on Nb surfaces do indeed translate to emission reduction and accompanying performance improvement in Nb RF cavities. Maximum benefits are realized from the highest temperature (1300-1350 C) heat treatment for 4 hours or longer. Intermediate-temperature treatments are less effective. Perhaps still higher temperatures will yield additional benefits. To carry out these treatments the development of a method to protect the RRR drop was crucial. It is also essential to rinse the heat treated surface, presumably to remove particulate contaminants inevitably introduced during the process of removing of the cavity from the furnace. Benefits of heat treatment are evident in several ways. For the one test of 1350°C HT carried out on a single-cell 3-GHz cavity, 70 MV/m was reached without significant emission. In 1.5-GHz single-cell cavities, RF surfaces reached a maximum field of 53 MV/m. The density of emitters between 30-40 MV/m is reduced by an order of magnitude. The emissive properties of individual emitters encountered are markedly altered; for example emitters with β values of 100 for HT surfaces have 2 orders of magnitude lower emission current than emitters with the same β value seen on CT surfaces. After He processing, Q values remain independent of field level up to 30 MV/m as compared to 20 MV/m for CT surfaces. Maximum fields up to 53 MV/m are accessible.

Heat treated surfaces can essentially withstand exposure to clean air and clean methanol and completely recover their best behavior after processing. Water exposure is more damaging but can also be remedied by He processing. At present chemical residues are believed responsible for the strong FE observed above 25 MV/m with chemically treated cavities. An alternative is minute impurities within the bulk Nb which are exposed after each chemical treatment. However, clean air, clean water and clean methanol are all exonerated from any role as dominant emitter sources.

With regard to the emission mechanism itself, there is strong evidence to implicate condensed gases. It is established that at least part of the benefits of He processing are derived from removal of condensates, as has been suspected for some time. New DC field emission experiments on gas conditioning suggest that ion implantation is another important mechanism that may play a role in He processing.

Past research on DC and RF field emission has paid off handsomely. We believe that continued efforts will be essential to close the remaining gap between potential and existing capabilities of Nb cavities.

Table 1.
RRR of Nb Used to Make Cavities Reported on in Fig. 1.

<u>Laboratory</u>	<u>RRR</u>	<u>Refs.</u>
CEBAF	150-400	2
CERN	110-210	3
CORNELL	150-450	4
DESY	100	5
KEK	115-170	6
SACLAY	150-170	7
WUPPERTAL	150-400	8

Table 2.
Surface Preparation of 1.5 GHz 1-cell Cornell Cavities

Chemical Treatment

Etch in 1,1,1 Acid mixture for 1 -10 minutes
 Rinse 3x with clean water ($\rho = 18 \text{ M}\Omega\text{-cm}$, LSI Class II*)
 Soak 45 minutes in 5% hydrogen peroxide with ultrasound
 Rinse 3x with clean water
 Soak 45 minutes in clean water with ultrasound
 Rinse 3x with clean water.
 Transport to Class 10-100 Clean Area
 Rinse 3x in clean methanol (LSI Class 1/2).
 Dry in horizontal position
 Seal ends

Heat Treatment

Install in Furnace in Class 100 Clean Room with Ti Box
 Bake at 800 C for 6 hours.
 Heat 1350 C for 4 - 8 hours.
 Pressure outside hot zone 2×10^{-7} Torr.
 Remove from furnace.

Soak in clean methanol with ultrasound for 1/2 hour.

Rinse with clean methanol.

Dry in horizontal position

Test.

* Following a proposed system of classification being slowly adopted for LSI semiconductor chemicals: G. Sielaff and N. Harder, "A Classification Model for Liquidborne Particles in Semiconductor Process Chemicals", *Microcontamination* 4, 1 (1986) pp. 43-8.

Acknowledgements

This work has been supported by the National Science Foundation with supplementary support from the US-Japan collaboration. We are grateful to the following for kindly providing latest information on laboratory activities: W. Weingarten, B. Aune, G. Mueller, R. Latham and O. Fischer. We are indebted to the following students for their vigorous participation: K. Gendreau, T. Flynn, K. Green, A. Liebovich, W. Hartung, J. Graber, S. Rubel, Eric Lochstedt. Many thanks are due to our technical support staff and especially to: Ron Prouty, Bill Edwards, Gerry Lawton, Tim Giles.

References

- [1] Proc. of the Third Workshop on RF Superconductivity, Argonne, Illinois, ANL-PHY-88-1 (Argonne National Lab, Argonne, IL, 1988, K. Shepard, Ed.)
- [2] H. Grunder, Proc. of the 1988 Linac Conference, Williamsburg, Va, October 1988.
- [3] W. Weingarten, Proc. of the XIII th International Symposium on Discharges and Electrical Insulation in Vacuum, Paris, 1988, p. 480., and priv. communication.
- [4] Q. S. Shu et al., Proc. of the 1989 Particle Accelerator Conference, Chicago, Illinois, March 1989.
- [5] D. Proch, Proc. of the 1988 Linac Conference, Williamsburg, Va, October 1988.
- [6] Y. Kojima et al., Proc. of the 1989 Particle Accelerator Conference, Chicago, Illinois, March 1989.
- [7] G. Mueller et. al, Proceedings of the European Particle Accelerator Conference, June 1988.
- G. Mueller et al, Proc. of the XIII th International Symposium on Discharges and Electrical Insulation in Vacuum, Paris, 1988, p. 480., B.Aune , Priv. communication
- [8] G. Mueller, Proceedings of the European Particle Accelerator Conference, June 1988, and priv. communication.

- [9] A. Citron, Proc. of the 1st Workshop on RF Superconductivity, KFK, Karlsruhe, 1980, KFK 3019, p. 3. Ed. M. Kuntze
- [10] D. Moffat, this workshop
- [11] B. Aune and G. Mueller, priv. communication
- [12] Ph. Niedermann, Thesis No. 2197, U. of Geneva, Geneva, Switzerland.
- [13] H. Padamsee, et al., 1987 Particle Accelerator Conference Proceedings, Washington, DC (March 1987), IEEE Cat. No. 87CH2387-9, p. 1824
- [14] H. Padamsee, et. al, Proc. of the Third Workshop on RF Superconductivity, Argonne, Illinois, ANL-PHY-88-1 (Argonne National Lab, Argonne, IL, 1988, K. Shepard, Ed.), p. 251
- [15] W. Weingarten, [1] Proc. of the Second Workshop on RF Superconductivity, CERN, p.551, E. H. Lengeler (1984)
- [16] See Refs. 3.
- [17] R. W. Roth, et. al, this workshop.
- [18] H. Padamsee, et al, SRF 850501 EXA, May 1985.
- [19] C. Lyneis, Proc. of the 1st Workshop on RF Superconductivity, KFK, Karlsruhe, 1980, KFK 3019, p. 119, Ed. M. Kuntze
- [20] Q. S. Shu, et al., IEEE Trans. Mag-25, 1868, 1989.
- [21] G. Loew et al., Proc. of the XIII th International Symposium on Discharges and Electrical Insulation in Vacuum, Paris, 1988, p. 480., and priv. communication., see also SLAC PUB 4647, May 1988.
- [22] C. B. Duke et al., J. Chem. Phys. Vol 46, p 923, 1967.
- [23] Q. S. Shu et. al, This workshop.
- [24] I. Campisi, et al., SLAC/AP-16, Feb 1984.
- [25] J. Graber, et al., This workshop.
- [26] Ph. Niederramn et al., Proc. of the XIII th International Symposium on Discharges and Electrical Insulation in Vacuum, Paris, 1988.
- [27] S. Bajic and R. Latham, J. Phys. D. (Appl. Phys.) 21 p. 943, (1988).